WILKINS, Eugene M., 1922–
AERODYNAMIC AND ELECTRODYNAMIC
PROCESSES IN TORNADOES.

The University of Oklahoma, Ph.D., 1963
Physics, meteorology

University Microfilms, Inc., Ann Arbor, Michigan

THE UNIVERSITY OF OKLAHOMA

GRADUATE COLLEGE

AERODYNAMIC AND ELECTRODYNAMIC PROCESSES IN TORNADOES

A DISSERTATION

SUBMITTED TO THE GRADUATE FACULTY

in partial fulfillment of the requirements for the

degree of

DOCTOR OF PHILOSOPHY

BY

EUGENE M. WILKINS

Norman, Oklahoma

1963

AERODYNAMIC AND ELECTRODYNAMIC PROCESSES

IN TORNADOES

APPROVED BY

Walter J. Saucier

C A Flint

Roy Fowler

Arthur Bernhart

William N. Huff

Yoshikazu Sasaki

DISSERTATION COMMITTEE

FOREWORD

A program of research was conducted in 1961 and 1962 to determine to what extent the electrical phenomena in thunderstorms might be effective in the genesis, maintenance, and intensification of a tornado. The investigation consisted entirely of laboratory experiments and theoretical analyses, although observational data on tornadoes were used to the extent that such data were available.

Special assumptions were imposed on the meteorological equations of motion in order to derive a three-dimensional vortex model having distributions of pressure and velocity that agree with those generally attributed to the tornado. This model is sufficiently simple mathematically that it can be used for analyses in the steady state and also for computing energy requirements during changes of state. The hydro-electrodynamic motion equations were then derived and particularized to the conditions imposed upon the model.

A vortex cage was constructed on a design to produce small vortices whose pressure and velocity patterns are similar to those of the theoretical model, and hence to the tornado. Similarity rules were then derived for the purpose of carrying over to the tornado the results of laboratory experiments testing the relative importance of aerodynamic, thermodynamic, and electrodynamic influences. The most important implications derivable from these studies are as follows:

1) Electrodynamic action is incapable of generating a tornado, and can exert no important influence on a tornado in the steady state.

2) The tornadoes that are observed to have a continuous electrical discharge inside may or may not be driven by the heat released from the discharge, but the vortex driven by discharge heat will be much weaker than the usual tornado. A characteristic difference in appearance of the two types is suggested and illustrated photographically.

3) The axis of a tornado may serve as a preferred path for discharging a thunderstorm, in which case the centrifuge action of the vortex does work against the thermally-expanding discharge column. The effect is to decrease the kinetic energy of the tornado by as much as 25 per cent.

4) An atmospheric vortex will form and grow vertically to boundaries if a zone of updraft is compensated by a tangentially-directed layer of air of arbitrary thickness, or a jet, located somewhere between the top and bottom of the updraft. The vortex thus formed is optimized when the inflow from this layer is symmetrical with respect to the updraft axis. The vortex takes on a tubular appearance as a result of asymmetry of inflow, and becomes progressively weaker and more tube-like with increasing asymmetry.

5) New evidence supports the older concept that tornadoes form by contraction of a microcyclone, but the energy requirements are

much greater than calculated previously. The direct processes are purely aerodynamic and thermodynamic.

This research was conducted under a grant to the University of Oklahoma Research Institute from the National Science Foundation. The advisory committee for the dissertation is Professor W. J. Saucier, Chairman, and Professors C. A. Plint, R. G. Fowler, A. F. Bernhart, W. N. Huff, and Y. Sasaki. The author is indebted to Professor Sasaki for guidance and inspiration beyond the usual functions of a dissertation advisor. Special thanks are due Professors R. G. Fowler, Sidney Corrigan, and Jack Cohn of the Physics Department and to Professor A. von Engel from Oxford for visiting the vortex laboratory to lend technical assistance and encouragement.

Gratitude is expressed to Professor C. M. Sliepcevich, Chairman, and to all members of the Graduate Standards Committee of the Engineering Sciences degree program. Through their guidance it was possible to select a program of studies in meteorology, engineering, physics, and mathematics appropriate to the multi-disciplined research program.

The Atmospheric Research Laboratory provided ideal quarters, services, and surroundings for the research in addition to the valuable associations with its personnel. Special mention is made of S. L. Barnes, who gave unselfishly of his time to photograph most of the experimental procedures, and to C. G. Clark for assistance in construction and repair of some laboratory equipment.

The program would not have been possible without the splendid cooperation of the author's employer, Ling-Temco-Vought, Inc., who made available several highly-specialized equipments in addition to contributing financial assistance. The author is grateful to Clyde Skeen, Executive Vice President and General Manager, for making it possible for him to pursue the program of graduate studies; these were beneficial to the research as well as personally rewarding. It is also pleasing to acknowledge the advice and assistance of Drs. F. W. Fenter, John Harkness and George Curtis of the Ling-Temco-Vought Research Center. Special thanks are due Messrs. E. L. Holcomb and L. T. McConnell of the Research Center for bringing the frequency spectrum analyzer to Norman and assisting with the discharge noise experiments.

TABLE OF CONTENTS

Chapter		Page

ILLUSTRATIONS

Figure		Page

AERODYNAMIC AND ELECTRODYNAMIC PROCESSES IN TORNADOES

Chapter I

INTRODUCTION

The electrical phenomena associated with thunderstorms in the locale of incipient tornadoes are often observed to have rather unusual characteristics with regard to visible displays and the frequency of lightning strokes. Occasionally a continuous electrical discharge is observed inside of the tornado itself. It is not surprising that Lucretius [18] (circa 60 B. C.) as well as numerous observers since that time have inquired as to what role the electrical phenomena might play in tornadoes of this kind. Recently Vonnegut [24] has speculated that thermal or electrodynamic accelerations may be important in the "electrical" tornado after it has formed by other means. Then Rathbun [21] hypothesized that tornadoes could be initiated by electrodynamic accelerations. Because these challenges were presented, their evaluation was required as a logical first step in research of a more important nature, namely that directed toward tornado control, forecasting, and surveillance.

Prior to the investigations of the present program there was no information on which an assessment of the role of electrical phenomena in tornadoes could be based. This was especially true in the science of meteorology, where the nature of electrical discharges in general and thunderstorm electrification in particular is very poorly understood. One might suppose that some calculations of the relative magnitudes of electrically-derived accelerations and aerodynamic accelerations could be made for a vortex by using the measurements of lightning stroke power and frequency reported in the literature. These could then be compared with pressure and centrifugal accelerations. But this would have required a suitable model for the distribution of the pressure and motion patterns in a tornado vortex, and no such model was available. The logical procedure at the inception of this program early in 1961 was to deduce such a model from theory and from the meager information available on tornadoes, to attempt to produce a similar vortex in the laboratory, and to study the model's characteristics in the steady state and during formation and decay. Following this, electrodynamic, thermal, and aerodynamic influences could be introduced to each state in order to seek for the relative importance of these influences. Finally, it was hoped that designs for further experiments directed toward tornado detection and control might evolve from the information gained.

The organization of the Table of Contents shows that the program has proceeded much the same as it was originally conceived. The necessity for a few of the experiments listed in the project proposal [30] was precluded by findings early in the program. Some laboratory model experiments along the line of tornado detection and control have been conducted and others are in progress. The results of this phase of the investigation will form the final report of the project as conducted under the present grant from National Science Foundation.

The reader will recognize that many of the analyses and the ensuing conclusions depend upon the theoretical model vortex derived, as well as upon the laboratory model. True fidelity to a natural atmospheric vortex could not be expected. Nevertheless the model is felt to be more complete with respect to the most important characteristics of a tornado than any derived previously. The object here, however, was not to excel in vortex mechanics, but to obtain a tool that would satisfy the needs of the research goals. The salient feature of the model for the purpose at hand is the fact that it proved useful in meeting the requirements for most of the major objectives of the program. For example, if it had proved to be impossible to use the same model for each of the analyses for model similarity, necessary and sufficient energy interchanges, and for evaluating the relative importance of processes, then there would have been little coherence in the final results. Such a lack of coherence would have limited severely the conclusions obtainable from the research.

A major difference in analysis technique exists between the vortex in a steady state and the vortex during changes of state. This provides the distinction between Chapters II and III, which form the main body of the text. Evaluations of aerodynamic, thermodynamic, and electrodynamic influences on these states, the major issues of the investigation, are carried within these chapters at places deemed appropriate for such evaluations. The conclusions in Chapter IV are overall conclusions, and not a repetition of the conclusions from individual experiments and analyses. This construction was used for the sake of conciseness.

At the outset of the investigation there was sufficient diversity of opinion on tornado genesis to permit complete objectivity in the comparison of aerodynamic, thermodynamic, and electrodynamic influences. There was no preference for any particular mechanism for tornado genesis until the roles of these influences began to be revealed from the vortex experiments and the researches into electrical theory. There is nothing sensational in the discovery that electrodynamic effects are not a direct factor in tornado genesis or maintenance. The importance of the discovery is as follows: 1) it answers questions posed by recent speculations in the literature; and 2) it narrows the scope of the effort toward tornado control. If in addition to these results the investigation also helps to improve our understanding of the concentrated atmospheric vortex, then the effort will have been most rewarding.

CHAPTER II

THE VORTEX IN THE STEADY STATE

Lamb [13] has stated that the fluid vortex is intractable in three dimensions, even with the grossly simplifying assumptions of the "perfect" fluids. In dealing with atmospheric vortices, however, the luxury of even these assumptions can hardly be afforded. There is little wonder, then, that so much is unknown about atmospheric vortices. Or stated more optimistically, it is remarkable how much we have learned about atmospheric vortices, considering their great complexity.

The purpose here is to deduce a suitable physical model for the velocity distribution within an atmospheric vortex on the scale of a tornado, whose radius varies from a few yards to several hundred yards. In piecing together this model we will utilize the meager knowledge existing from tornado observations and the calculations afforded from theoretical considerations to the extent that the two can be brought to agreement. In addition we wish to establish the dynamic similarity, if any, between a vortex generated by special apparatus in the laboratory and a real tornado, recognizing that both model and tornado are subject to a variety of types. The apparatus and general features of vortices generated therewith have been discussed in an earlier project report [31].

The laboratory vortex has an average diameter of about one inch, and is slightly larger at the top than at the bottom. This diameter is actually based on the sharply defined "sleeve", which is quite similar in appearance to that of a tornado. However, just as in the case of the tornado, the exact reason for this sharp boundary is unknown. We will see later that it is not the same as the sleeve of maximum velocity. A feature of the laboratory vortex generally considered common to tornadoes and other atmospheric vortices, is a radial profile of tangential velocity v_θ with zero at the center, a maximum velocity v_m at some radial distance r_m, and decreasing again to zero (or to a negligible value, indistinguishable as part of the vortex) at some distance r_o. The regions on either side of r_m are identified here as I and II respectively.

The laboratory vortex cage is equipped to measure the pressure drop at the center of the vortex, and we wish to relate this pressure drop to the maximum tangential velocity, or "sleeve" velocity, v_m. Further, by similarity analysis, we hope to relate these same pressure-velocity characteristics to those in a tornado for use in the interpretation of other vortex experiments.

The integrals of the velocity profiles will always be expressible in terms of maximum velocity, and the pressure drop, Δp, will thus also be expressible in terms of maximum velocity. Establishment of similarity rules will then allow comparison of vortex characteristics on a laboratory scale with those of a larger scale by using only the Euler number and the parameters of major interest.

The vital but little understood process of energy transformation in vortices will be discussed later. The vertical motion scheme, long known to be of major importance in all atmospheric vortices, and also verified as vital to liquid vortices by Long [16], will be discussed only qualitatively at first, and later formulated to agree with conditions imposed on the model.

The method of attack will be to begin with the complete set of motion equations basic to dynamic meteorology. These will be converted to cylindrical coordinates in order to take advantage of the properties of model shape. Solutions will be sought that are agreeable to the special requirements. We will keep track of the consequences of the various simplifying assumptions in order fully to realize our departures from reality and the significance of these departures.

For one reason or another, only a few of the results of previous investigations in vortex mechanics and model experiments have been found useful for the purpose at hand--this despite the rich background of information available in the literature. However, without knowledge of these earlier efforts no logical starting point would be found. A more complete bibliography on the subject is given in a report prepared at the beginning of this project [30].

Motion Equations for a Model Vortex

Beginning with the meteorological equations of motion, complete except for surface friction, which will be discussed qualitatively later, we have

$$\frac{d\vec{V}}{dt} = -\frac{1}{\rho}\nabla p - 2\Omega \times \vec{V} - \vec{g} - \nu\nabla^2\vec{V}. \qquad (1)$$

We resolve this equation along cartesian axes and convert to cylindrical coordinates to obtain the relations

$$A + D - G - J = 0,\ B + E - H - K = 0, \text{ and}$$

$$C + F - I - L = 0, \qquad (2)$$

where

$A = \frac{\partial v_r}{\partial t}$ ---------------------------- radial acceleration

$B = \frac{\partial v_\theta}{\partial t}$ ---------------------------- tangential " (3)

$C = \frac{\partial w}{\partial t}$ ---------------------------- vertical "

$D = \left[v_r\frac{\partial}{\partial r} + \frac{v_\theta}{r}\frac{\partial}{\partial \theta} + w\frac{\partial}{\partial z}\right]v_r - \frac{v_\theta^2}{r}$ ---- advection and radial acceleration

$E = \left[v_r\frac{\partial}{\partial r} + \frac{v_\theta}{r}\frac{\partial}{\partial \theta} + w\frac{\partial}{\partial z}\right]v_\theta + \frac{v_\theta v_r}{r}$ -- advection and tangential acceleration

$F = \left[v_r\frac{\partial}{\partial r} + \frac{v_\theta}{r}\frac{\partial}{\partial \theta} + w\frac{\partial}{\partial z}\right]w$ ---------- advection and vertical acceleration

$G = fv_\theta - \frac{1}{\rho}\frac{\partial p}{\partial r}$ ------------------------- Coriolis and pressure accelerations

$H = -fv_r - \frac{1}{\rho r}\frac{\partial p}{\partial \theta}$ -------------------- Coriolis and pressure accelerations

$I = -\frac{1}{\rho}\frac{\partial p}{\partial z} - g$ ------------------------- pressure and gravity accelerations

$$\left.\begin{aligned} J &= \nu\nabla^2 v_\Theta \\ K &= \nu\nabla^2 v_r \\ L &= \nu\nabla^2 w \end{aligned}\right\} \text{--------------------viscous (shear) force per unit mass.}$$

The notation is standard for dynamic meteorology unless otherwise specified. The Laplacian operator here is the usual one for cylindrical coordinates. Only those Coriolis terms that are customarily ignored are omitted here. We observe the convention that

$$v_r = \frac{\partial r}{\partial t}, \ \frac{v_\Theta}{r} = \frac{\partial \Theta}{\partial t}.$$

The conditions stated in (1) result from the coordinate transformation, and they may be satisfied in a variety of ways. The equations are satisfied either by having the terms in (1) vanish individually, which involves special assumptions, or else they must vanish in the sum, which gives the complete meteorological equations of motion in cylindrical coordinates. The equivalents of the capital letters are given in set (3).

Special Assumptions

First we assume a steady-state situation, since the interest here is in the pressure and velocity structure while the vortex is not growing or dissipating. This means A = B = C = 0.

Now the laboratory vortex tends to retain circular symmetry if air enters tangentially equally from each side of the cage. Doubtless the assumption of circular symmetry in the distribution of the dependent variables velocity and pressure is also a fair one for some tornadoes in the steady state. This gives $\frac{\partial}{\partial \theta} = 0$.

The next assumption is that the viscous terms can be neglected. The justification is obvious in the case of a tornado, and was shown also to hold for the laboratory vortex in an earlier project report [31]. For similar reasons we can neglect the Coriolis accelerations. These terms are very small in any vortex, even when they are active in determining the initial direction of rotation.

The expression for the vertical component of vorticity is

$$\frac{\partial v_\theta}{\partial r} + \frac{v_\theta}{r} = \zeta, \qquad (4)$$

The vanishing of ζ is the necessary and sufficient condition for the existence of a velocity potential. Integration of (4) with $\zeta = 0$ gives the formula for the velocity profile of the well-known irrotational vortex, $v_\theta r = \text{const}$. Irrotational motion is not acceptable in region I of the vortex model, since we seek $v_\theta = 0$ at the vortex center, and not $v_\theta = \infty$. If irrotational motion is accepted for region II, then we have the problem of defining r_o, the radius at the outer limit of the vortex.

Properties of the Model

The equations of motion now are

$$\left[v_r \frac{\partial}{\partial r} + w \frac{\partial}{\partial z} \right] v_r - \frac{v_\theta^2}{r} = -\frac{1}{\rho}\frac{\partial p}{\partial r}$$

$$\left[v_r \frac{\partial}{\partial_r} + w \frac{\partial}{\partial z} \right] v_\Theta + \frac{v_\Theta v_r}{r} = 0 \qquad (5)$$

$$\left[v_r \frac{\partial}{\partial r} + w \frac{\partial}{\partial z} \right] w = - \frac{1}{\rho} \frac{\partial p}{\partial z} - g.$$

The second of these may be written

$$\zeta = - \frac{w}{v_r} \frac{\partial v_\Theta}{\partial z} , \qquad (6)$$

which gives the vorticity as a function of the vertical distribution of vortex intensity. The vortex is irrotational in a region where the intensity is constant with height. Since v_r is negative and w positive for radial inflow, cyclonic vorticity exists where the vortex intensity increases with height, and anticyclonic vorticity where it decreases with height.

If we consider region II separately, it is possible that radial inflow there could exist with negligible vertical motion. With this assumption we set w = 0 in (5) to obtain

$$v_r \frac{\partial v_r}{\partial r} - \frac{v_\Theta^2}{r} = - \frac{1}{\rho} \frac{\partial p}{\partial r} \qquad (7)$$

$$\frac{\partial v_\Theta}{\partial r} + \frac{v_\Theta}{r} = \zeta = 0 \qquad \text{(irrotational motion)}$$

$$0 = -\frac{\partial p}{\partial z} - \rho g . \qquad \text{(hydrostatic equilibrium)}$$

Combining the first pair, we obtain

$$v_r \frac{\partial v_r}{\partial r} + v_\Theta \frac{\partial v_\Theta}{\partial r} = - \frac{1}{\rho} \frac{\partial p}{\partial r} \qquad (8)$$

or $$-d\left[\frac{v_r^2}{2}+\frac{v_\theta^2}{2}\right]=\frac{dp}{\rho}.$$

If density is assumed constant through the region, the pressure drop is easily related to the total kinetic energy of horizontal motion in the region.

In region I of the model we will specify that $v_r = 0$, in which case continuity requires that $\frac{\partial w}{\partial z} = 0$, and we obtain the equations of horizontal motion from (5) as follows:

$$\frac{v_\theta^2}{r} = \frac{1}{\rho}\frac{\partial p}{\partial r} \qquad \text{(cyclostrophic flow)}$$

$$\frac{\partial v_\theta}{\partial z} = 0 \qquad \text{(intensity constant with height)} \qquad (9)$$

$$0 = -\frac{1}{\rho}\frac{\partial p}{\partial z} - g. \qquad \text{(hydrostatic equilibrium)}$$

Irrotational motion is required for the zone having radial inflow since this is the only motion scheme which will allow the profile of v_θ to remain unchanged (steady state) when the process of angular momentum conservation is operating on the air parcels as they move toward smaller radii in the vortex. Thus the simpler solutions indicate irrotational motion as the most reasonable assumption that we can make for region II.

The set (9) is more applicable to region I where we would suppose w to be greater than v_r, because the air entrained into I from II must be exhausted vertically. This set predicts that the vortex intensity will not vary with height, but does not predict the form of the radial profile of tangential velocity. Note that there are no restrictions on vorticity in region I.

We are left without a prediction for the distribution of tangential velocity in region I and without a prediction for the vertical distribution of vortex intensity in region II. We will attempt to infer these later from separate considerations.

Consider the vorticity equation for a circular vortex

$$\frac{\partial v_\theta}{\partial r} + \frac{v_\theta}{r} = \zeta(r),$$

which may be expressed as

$$v_\theta r_m = \int_0^{r_m} \zeta(r)\, r dr \qquad (10)$$

for region I. This gives the desired velocity profile if we can assume a logical form for the radial profile of vorticity in region I. Now consider the following situations: 1) ζ = constant $\neq 0$. This gives v_θ = const x r_m, which is constant velocity. 2) $\zeta = \zeta(r)$. Regardless of the functional form of $\zeta(r)$, the integrand becomes constant when evaluated at the limits, giving constant velocity throughout the region. This is not acceptable. Now suppose we express (10) as follows:

$$v_\theta r = \int_0^{r} \zeta(r)\, r dr \quad (r < r_m), \qquad (11)$$

ζ = const. gives $v_\Theta = \frac{\zeta r}{2}$, which is solid rotation, and $\zeta = 2\omega$. There are few restrictions on the functional form for $\zeta(r)$ as long as the integration does not proceed to a definite value of r. This means that we may consider some zone of unspecified dimensions to exist between regions I and II to permit a transition from the irrotational motion of region II to any motion system whatsoever in region I, where the tangential velocity is zero at the center and increases outward.

This transitional zone, of course, is where the radial inflow is changing to vertical updraft. Within this zone neither w nor v_r is negligible, and the set of equations (5) must apply. The thickness of the transition zone evidently depends on the volume rate of radial inflow relative to the vortex dimensions. This zone has several other interesting properties:

1) The maximum tangential speed v_m occurs there, since angular momentum is conserved up to the point that $v_r = 0$.

2) Due to streamlines curving from horizontal to vertical there is a centrifugal acceleration there directed toward the center of the vortex and downward.

3) The centrifugal term $\frac{v_\Theta^2}{r}$ is greatest in this zone. There is no requirement for a cyclostrophic balance in the transition zone (neither set (7) nor set (9) applies except at the boundaries). We can speculate that the profile of tangential velocity most resembles region I in its inner half and region II in its outer half.

4) Equation (6) applies in the transition zone, where w and v_r are about the same order of magnitude. Unless we follow the assumption that the transition zone is negligibly thin, only overlapping slightly in each region, we are faced with the consequence that the vortex intensity increases with height if the vorticity is cyclonic there. If we want the velocity profiles in each region to join at v_m, then we must have $\frac{\partial v_\theta}{\partial z} > 0$ in each region also. But from (9) we saw that this is forbidden in region I. We must therefore prefer to consider the transition zone negligibly thin when integrating the complete velocity profile.

5) A reasonable picture of the transition of flow from region II to region I is one in which r_m increases with height, i. e., the transition zone is funnel-shaped, as shown in Fig. 1. This is a logical streamline pattern that will permit the transition from horizontal to vertical flow to take place within a zone of minimum thickness.

Aside from serving as an exhaust duct for the radial inflow, region I serves no particular function as far as tangential velocity component is concerned. The region might as well be regarded as an idler, or cylinder in solid rotation, with the tangential component being applied to it at r_m. The exception is found near the ground, or lower boundary, where friction acts. If the rotation in region I is solid, then viscous forces can act only at the surface.

The model finally selected has the radial profile of tangential velocity similar to the vortex sometimes called the Rankine combined

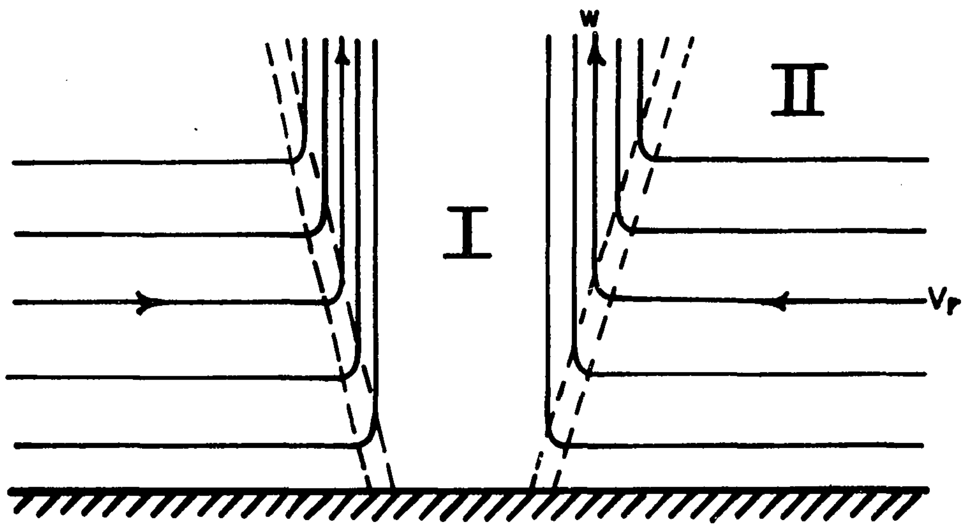

Figure I. Cross-section of vortex model showing zone of transition from horizontal component of flow in region II to vertical in region I.

vortex. It has been used as a model in the discussion of dust devils by Flower [7] and by Battan [1], and for the discussion of tornadoes by Fulks [9]. Hill [11], Love [17], and Lamb [13] (op. cit., p. 29) have used this model for problems in fluid mechanics. To the author's knowledge neither the justification for its selection nor the consequences of the various assumptions leading to this model has been set forth previously. The difference between this model and the classic one is that r_m increases with height due to taking into account the transition zone. It also differs in that a radial velocity component exists in region II. In the classic model the vertical dimension is disregarded entirely. We may still take advantage of the classic model's simplicity by analyzing a horizontal slice through the vortex at some arbitrary level between the top of the friction layer and the top of the vortex. Pressure and horizontal velocity profiles for the model are shown schematically in Fig. 2.

The tangential velocities by regions are related to v_m by the equations

$$v_I = \frac{v_m r}{r_m} \qquad v_{II} = \frac{v_m r_m}{r} \quad . \tag{12}$$

Surface Friction

The effect of surface friction is seen by taking $v_r = -kv_\theta$ where k is the coefficient of surface friction. The interpretation is that a radial component inward results from slowing the tangential velocity

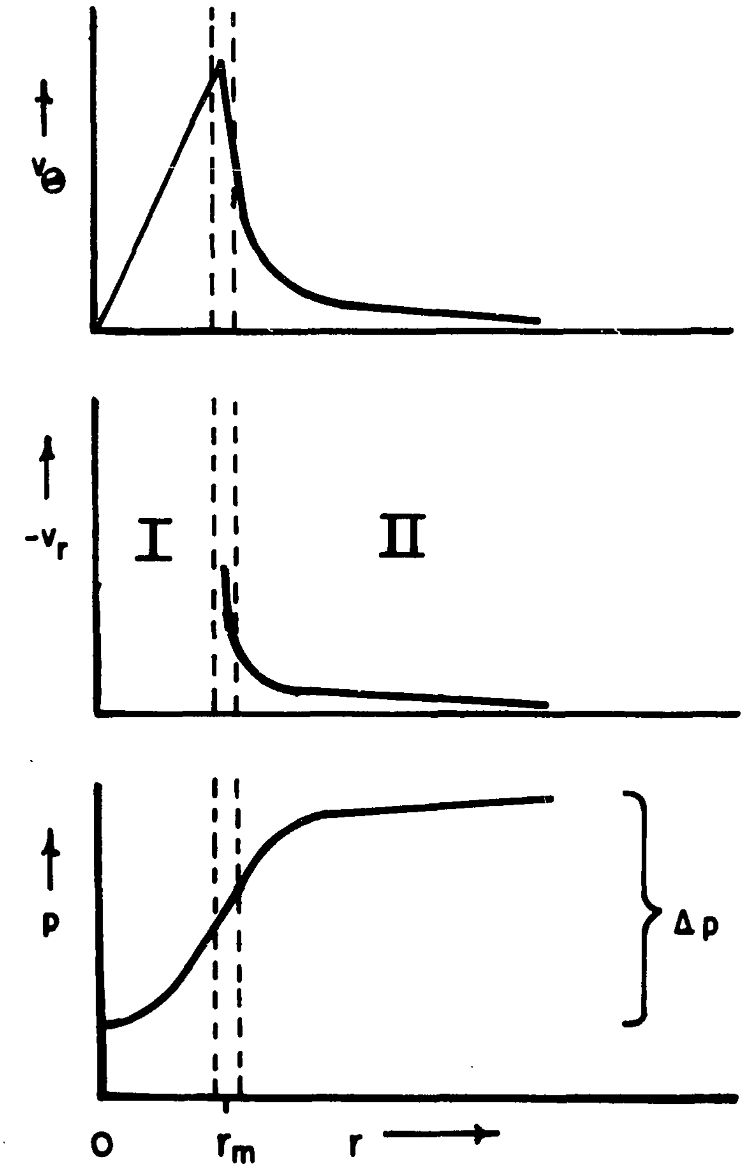

Figure 2. Radial profiles of tangential velocity, v_θ, radial velocity, v_r, and pressure in the vortex model.

component below the point where the centrifugal acceleration balances the pressure gradient. The horizontal convergence thus produced in the boundary layer may be expressed as

$$\mathrm{Div}_f\, V = \frac{\partial v_r}{\partial r} + \frac{v_r}{r} = -k\left[\frac{\partial v_\Theta}{\partial r} + \frac{v_\Theta}{r}\right] = -k\zeta\,. \qquad (13)$$

The magnitude of the frictionally induced convergence is thus seen to be related to the vorticity. The conditions required for the model vortex do not hold for the friction layer, and the velocities v_r and v_Θ in (13) are understood to apply only in the friction layer. This shows that the friction layer must be excluded from consideration in the model, otherwise we would have frictionally induced convergence of magnitude $2\,\omega k$ in region I and zero in region II. This would be a contradiction to the condition desired for the model, namely that radial inflow occur in region II but not in region I.

Relation between Radial Inflow and Updraft

The relation between v_r and w for incompressible flow in the vortex model may be found by using a purely geometric analysis. We find the expression for the inflow rate in region II, and equate it to the exhaust rate in region I. Figure 3 is a diagram of the quantities used to calculate the relationship desired.

Consider that the radial inflow occurs in a horizontal slab of thickness dz. The value of v_r reaches a maximum v_{rm} at the radius r_m, which is the radius of the sleeve of maximum vortex inten-

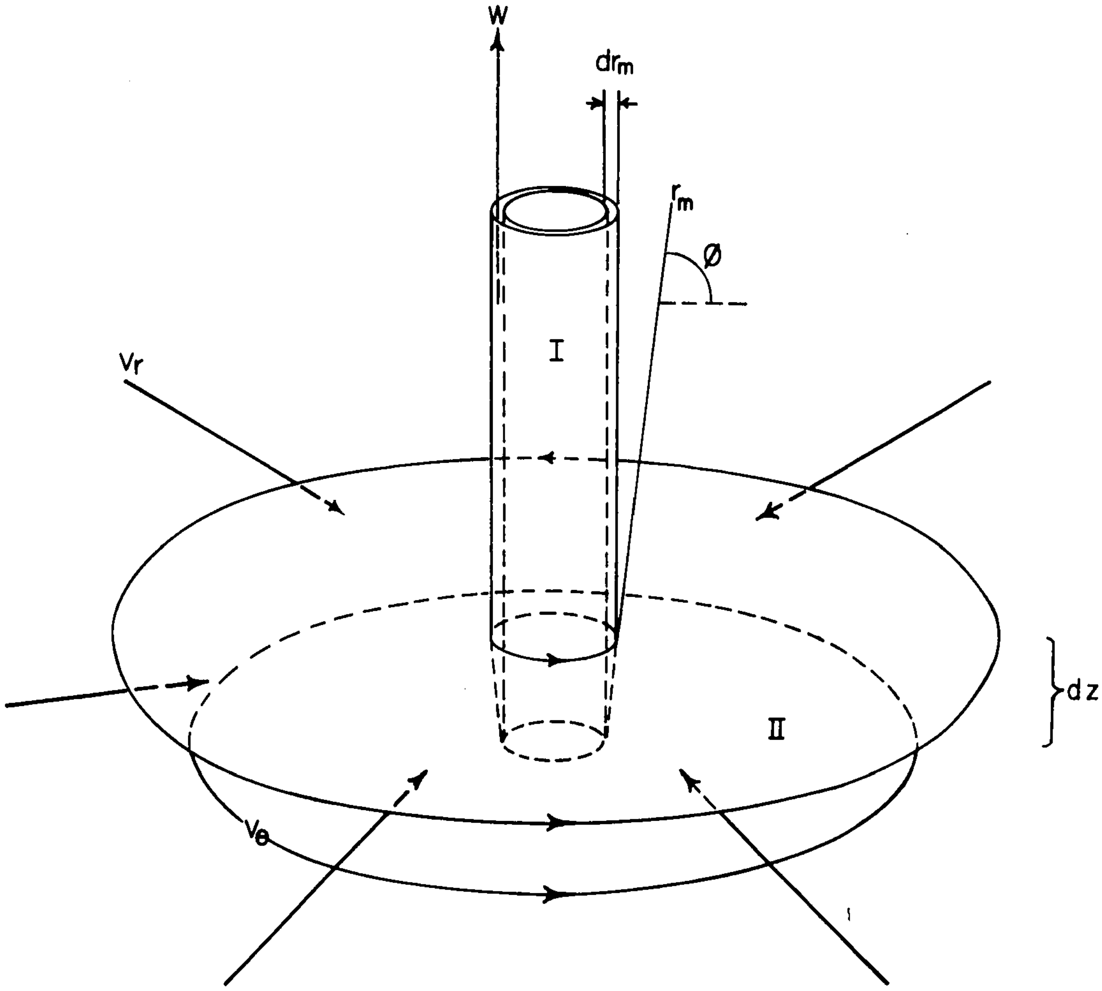

Figure 3. Diagram of the quantities used to determine the relationship between radial inflow, v_r, and updraft, w, in the model vortex.

sity within the slab of thickness dz. Recall that this model allows r_m to increase with height if air is discharged vertically upward in region I. The horizontal flow through the slab is $2\pi r_m dz\ v_{rm}$. Within the narrow funnel-shaped region called the transition zone the non-tangential component of the flow changes from horizontal to vertical as depicted in Fig. 2, but all the while the rotational velocity component v_θ continues. The vertical component of flow is contained in a cylindrical sleeve of thickness dr_m, and the cross-section area element dA of the updraft is $2\pi r_m dr_m$. The vertical flow rate then is $2\pi r_m\ dr_m\ w$. Equating the two flows gives

$$\frac{w}{v_{rm}} = \frac{dz}{dr_m} \quad . \tag{14}$$

Thus we see that v_{rm} and w are related by the slope of the sleeve of maximum vortex intensity. In the simple case where this sleeve has the shape of an inverted cone, v_{rm} and w differ only by a constant, and if v_{rm} is constant or varies linearly with height, then w will be constant or vary linearly with vortex radius.

The relationship may also be solved for a variety of sleeve shapes where the sleeve is definable as a surface of revolution. Suppose, for example, that the sleeve is a paraboloid of revolution branching radially with apex at the ground, and that r_{mo} is where the sleeve intersects the ground. The equation of the sleeve is

and
$$z^2 = 8r_{mo}(r_m - r_{mo})$$
$$\frac{dz}{dr_m} = \frac{4r_{mo}}{z} \qquad (15)$$

so that
$$w = \frac{4r_{mo} v_{rm}}{z} = v_{rm}\left[\frac{2r_{mo}}{r_m - r_{mo}}\right]^{\frac{1}{2}}.$$

This gives sufficient relationships to specify the radial distribution of w. To avoid infinite updraft velocity at the surface we would require $v_{rm} = 0$ at the surface. At any rate, we see that the parabolic sleeve in this case would give a "jet-like" character to the updraft, i. e., higher velocities near r_{mo} and decreasing radially in proportion to the square root of the distance. The parabolic sleeve is analyzed here only to serve as an example, for there is no indication that atmospheric vortices have this characteristic.

In developing the model, the assumption that $v_r = 0$ in region I gave the result that $\frac{\partial v_\theta}{\partial z} = 0$ in the equations of motion. This requirement must also be met in region II in order that the maximum tangential velocity v_m will be common to both regions. The restriction on shear of tangential velocity can be removed for the purpose of treating a similar model in which the intensity varies with height. Such a refinement is not required for the problem at hand, but may be of interest for other applications. For this case v_θ will vary along r_m and we write

$$\frac{dv_I}{dr_m} = \frac{\partial v_I}{\partial r} + \frac{\partial v_I}{\partial z}\frac{dz}{dr_m} = \frac{v_m}{r_m} + \frac{\partial v_I}{\partial z}\frac{dz}{dr_m},$$

and similarly

$$\frac{dv_{II}}{dr_m} = \frac{-v_m r_m}{r^2} + \frac{\partial v_{II}}{\partial z}\frac{dz}{dr_m}.$$

Since $\frac{dv_I}{dr_m} = \frac{dv_{II}}{dr_m}$, we have

$$\left[\frac{\partial v_{II}}{\partial z} - \frac{\partial v_I}{\partial z}\right]\frac{dz}{dr_m} = \omega\left[\frac{r^2 + r_m^2}{r^2}\right],$$ where it is understood that r is the radius in region II at which $\frac{\partial v_{II}}{\partial z}$ occurs. Note also that when $\frac{\partial v_I}{\partial z}$ is specified, the vertical variation of vortex intensity may be calculated easily for any vortex whose sleeve of maximum velocity is expressible as a surface of revolution.

We now have sufficient relationships to specify completely the field of horizontal and vertical motion for a model vortex. With this accomplished we proceed with the investigation of the other properties of the model.

Pressure Drop

As stated earlier, we will require a relationship between the maximum tangential velocity v_m and the pressure drop between the vortex center and ambient in order to compare the vortex model with tornadic vortices.

Comparing equation sets (7) and (9) we see that the pressure drop is to be calculated by different methods in each region. The cyclostrophic assumption holds in region I, thus from (9) and

$v_I = \frac{v_m r}{r_m}$,

$$\Delta p_I \doteq \int_0^{r_m} \bar{\rho} v_I^2 \frac{dr}{r} = \bar{\rho} \int_0^{r_m} \frac{v_m^2}{r_m^2} r \, dr = \frac{\bar{\rho} v_m^2}{2} \qquad (16)$$

if we neglect density changes along r.

Equation (8) tells us that in region II we can relate the pressure drop to the total kinetic energy of horizontal motion, or

$$-\Delta p_{II} = \bar{\rho}\, d \left[\frac{v_r^2}{2} + \frac{v_{II}^2}{2}\right] \quad (r > r_m)\,.$$

To see how v_r varies along r, consider that it must increase inward as the area of the vortex cylinder decreases inward. In keeping with the assumption of constant density,

$$\frac{v_r}{v_{rm}} = \frac{2\pi r_m h}{2\pi r h}\,, \quad \text{or } v_r = \frac{v_{rm}\, r_m}{r}\,,$$

where h is the height of the cylinder of converging air. Thus we see that v_r obeys the same law as v_θ in region II, so that from equation (8) we obtain

$$-\Delta p_{II} \approx \frac{\bar{\rho} r_m^2}{2} \int_{r_m}^{\infty} d \left[\frac{v_{rm}^2}{r^2} + \frac{v_m^2}{r^2} \right]$$

or $$\Delta p_{II} = \frac{\bar{\rho}}{2} \left[v_{rm}^2 + v_m^2 \right] . \qquad (17)$$

The total pressure drop is

$$\Delta p = \Delta p_I + \Delta p_{II} = \bar{\rho} \left[v_m^2 + \frac{v_{rm}^2}{2} \right] . \qquad (18)$$

The integration may be carried to some arbitrary radius r_o instead of to infinity, if preferred.

The total pressure drop is equal to the kinetic energy of the maximum radial velocity component plus twice the kinetic energy of the maximum tangential velocity component.

This type of steady-state vortex requires only sufficient radial inflow to maintain the velocity profile in region II through the process of angular momentum conservation. Essentially this means overcoming the relatively small viscous forces. The model calls for transition of radial flow to vertical flow between regions I and II, so that v_{rm} can be estimated if the vertical flow rate is known, and this is easily accomplished for the laboratory vortex. This completes the first step in preparation for the similarity analysis, namely that of specifying the tangential velocity field in terms of pressure drop and other parameters easily measured in the laboratory vortex.

Radial Inflow Factor

The next step is to compare the model with the tornado. Because of the rather wide variety of tornado types, we will acknowledge at the beginning that this analysis applies only to a tornado having a velocity field similar to the model. The missing link is the value to use for the radial velocity component v_{rm} for region II of the tornado. We noted earlier that v_r and v_{II} vary inversely with r, and thus

$$\frac{v_r}{v_{II}} = \frac{v_{rm}}{v_m} = K, \qquad (19)$$

where K is a "radial inflow factor", constant at any point in region II during the steady state. In practice this factor may prove difficult to measure in the vicinity of a tornado, since it requires a wind reading at the precise moment that the center of the tornado can be ascertained. But the calculation is facilitated by the fact that the measurement need not be made in especially strong winds, as long as the flow is definitely associated with the tornado. This is because K theoretically is constant throughout the region.

Equation (18) can now be written in dimensionless form as

$$\frac{\bar{\rho} v_m{}^2}{\Delta p} = \frac{2}{2 + K^2} = E^2, \qquad (20)$$

where E is the Euler number. For the purpose of dynamic similitude we require that

$$E\,(\text{model}) = E\,(\text{tornado})$$

in which case

$$\frac{v_m \text{ (tornado)}}{v_m \text{ (model)}} = \left[\frac{\Delta p \text{ (tornado)}}{\Delta p \text{ (model)}}\right]^{\frac{1}{2}}, \qquad (21)$$

provided that the K factor is the same for each, or else is negligibly small.

It is easily seen that neglect of the K factor amounts to relating v_m to pressure drop by use of the cyclostrophic assumption, a common practice among investigators who have used a similar vortex model for the calculation of such relationships. The magnitude of the error as a function of K is shown in Fig. 4. The extreme case may be regarded as that in which K = 1 (radial and tangential components equal) giving v_m 18.4 per cent too large for a given pressure drop. In discussing tornadoes we are mainly interested in a maximum resultant velocity V, which is the vector sum of v_m and v_{rm}, or

$$V^2 = v_m^{\ 2} + v_{rm}^{\ 2} = v_m^{\ 2}\,(1 + K^2). \qquad (22)$$

The cyclostrophic approximation is satisfactory for region II alone, as long as it is understood that V is intended instead of v_m. However, this has no practical use, since it would require that Δp be measured at the point of maximum velocity. This would be most difficult, if not impossible. Clearly the cyclostrophic assumption cannot be used to estimate correctly any component of vortex velocity from vortex total pressure drop. However, where this has been done,

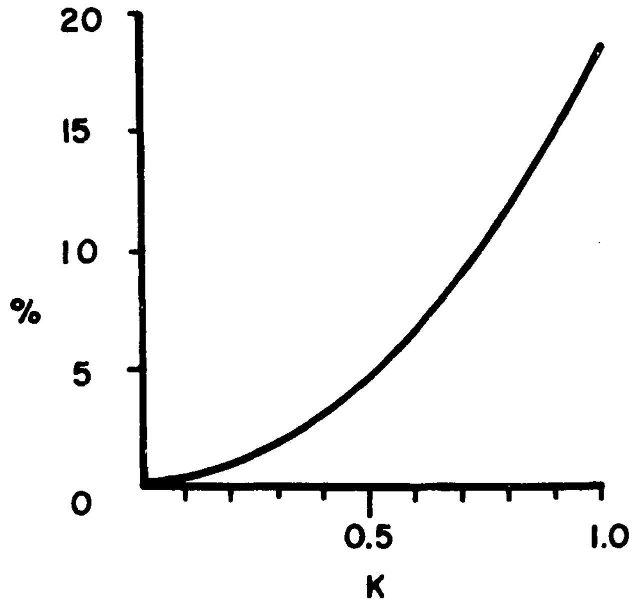

Figure 4. Per cent error in cyclostrophic approximation as a function of K-factor for the model vortex.

the v_m values so calculated may be corrected upon multiplying by the

$$\text{correction factor} = \left[\frac{1}{2 + K^2}\right]^{\frac{1}{2}} \quad . \qquad (23)$$

It may be that K is sometimes fairly small in a tornado, but K can never be zero in a steady-state vortex of this type, and it seems reasonably certain that is not negligible.

In one experiment with the optimized laboratory vortex it was found that K = 0, 36 for all pressure drops between 0.5 and 3.6 cm H_2O, corresponding to maximum tangential velocities ranging from 13.9 mph to 38.0 mph. The maximum resultant velocities corresponding to this situation are 14.8 mph and 40.3 mph respectively. The density $\bar{\rho}$ is taken as 1.3×10^{-3}g cm^{-3}for this calculation.

The cyclostrophic assumption would have given 14.3 mph and 39.0 mph. These values are not correct for either tangential or resultant velocities. While the error is not very large in this case, it could be considerable for larger K factors.

If the larger pressure drop of 3.6 cm H_2O with a resultant velocity of 40.3 mph is assumed to correspond to the largest pressure drop ever reported for a tornado, which is 0.2 atmospheres, then from equations (21) and (22)

$$\frac{V\ (\text{tornado})}{V\ (\text{model})} = \left[\frac{0.2}{0.0035}\right]^{\frac{1}{2}} = 7.58;$$

which gives V (tornado) = 305 mph. This is a reasonable approximation, and will be used later as the velocity scale factor for certain comparisons between model and tornado.

Velocity Distribution in the Experimental Vortex

Equation (20) gives the relationship between vortex total pressure drop and maximum tangential velocity for the model vortex. This equation is graphed in Fig. 5. The four experimental data points were measured in the vortex cage for a fast vortex (Δp = 36 mm H_2O) and a slow vortex (Δp = 14 mm H_2O) and for K = 0.36. The velocity instrumentation consisted of a stagnation pressure probe, or pitot tube, and a small "cup" anemometer, which are shown in Fig. 6. Each of these instruments was specially constructed for measurements in the vortex cage. The instruments were calibrated against a standard stagnation pressure velometer. A Meriam oil manometer was used with the pressure probe, and a stroboscope was used to time the speed of the anemometer.

Radial profiles of air speed were measured by each instrument in the region of the vortex to which it is best suited. The pressure probe is unsuitable at vortex radii less than one inch, since the probe itself is 0.5 in wide, and disturbs the vortex excessively at small radii. The pressure probe is not useful for velocities less than about 7 mph. The practical limitation of the anemometer was between radii of 0.25 in and 1.5 in. At larger radii the drag on the cup arms becomes significant, and at smaller radii the diameter of the cups

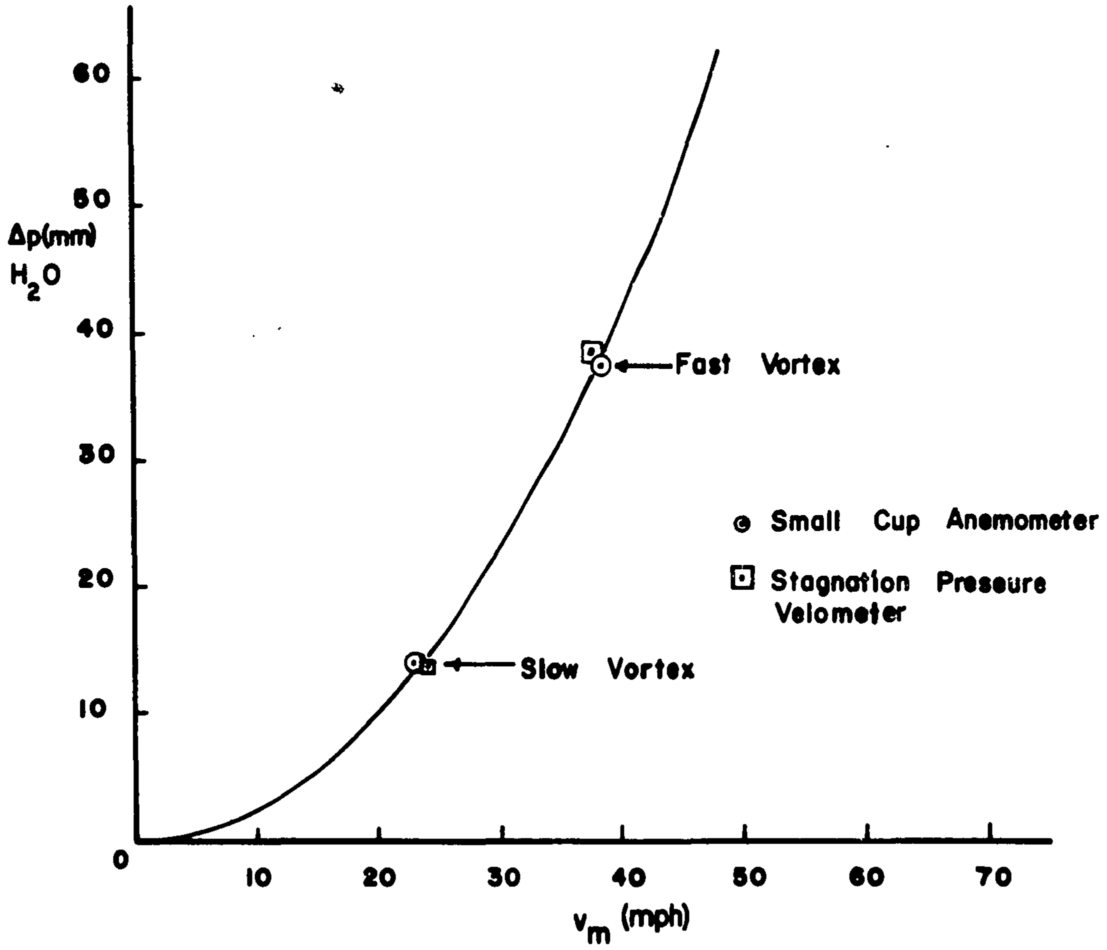

Fig. 5 Theoretical curve of v_m vs. Δp for the laboratory vortex for K-factor = 0.36.

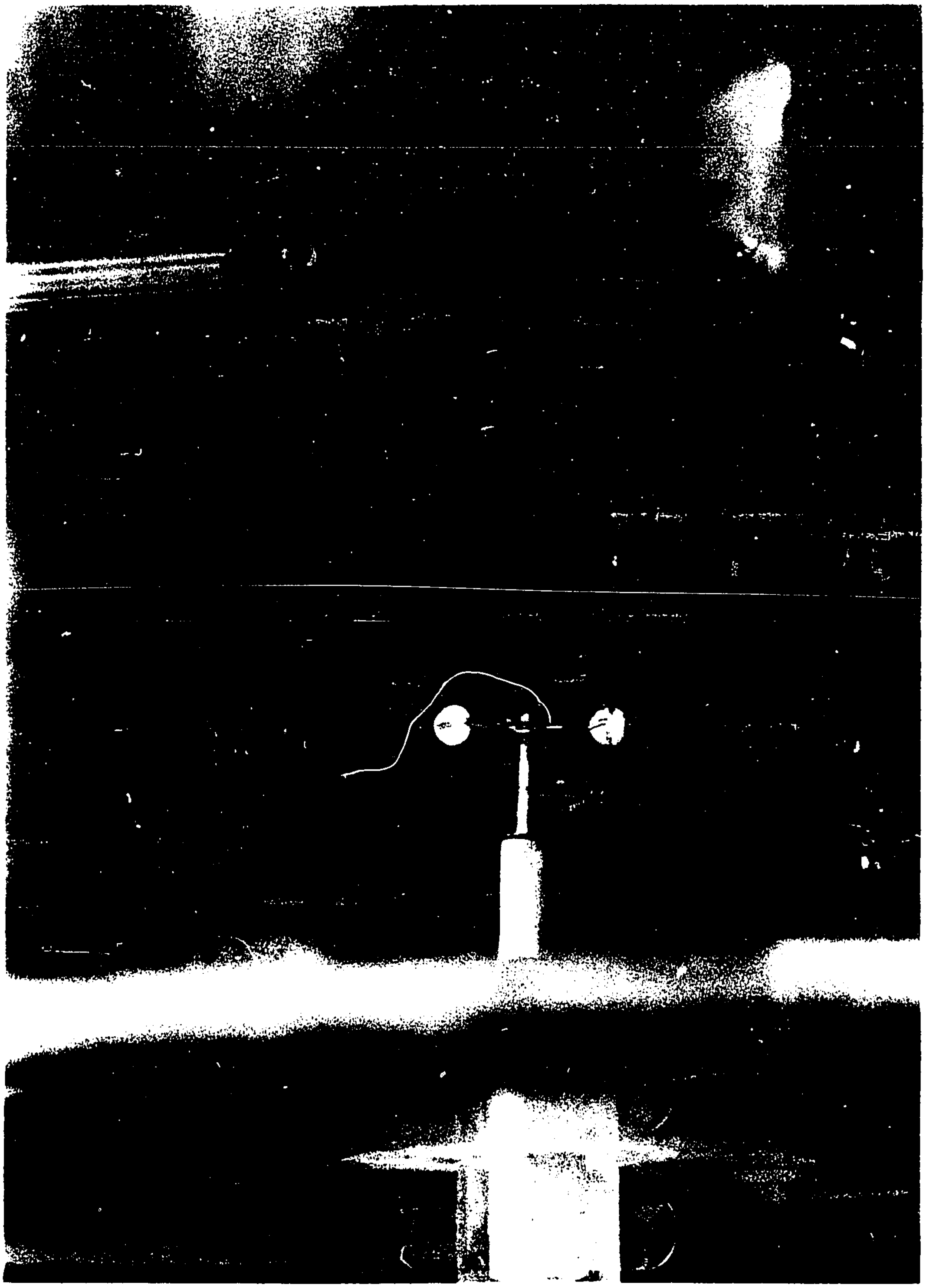

Fig. 6. Stagnation pressure probe and small anemometer used for measuring velocities in the laboratory vortex.

(0. 2 in) is the limiting factor. The cup anemometer was centered in the cage, and measurements at different radii were made by adjusting the lengths of the cup arms.

Figs. 7 and 8 give measurements of the radial profiles of tangential and vertical velocity for the fast and slow vortices, respectively. The theoretical curves, based on the model vortex, are drawn for comparison. The agreement is best at the radius of maximum velocity, but is also fair at greater radii. Actually, the data points correspond more closely to the resultant velocities, according to equation (22), than to the tangential velocities. This is shown by the dash lines in Figs. 7 and 8. Of course, this is what would be expected from the type of instrumentation used. Individual data points are reproducible to the nearest 0. 5 mph, so that the discrepancy may not be attributed to lack of precision in measurement. The curve of the data points has the shape of the theoretical curve, so we can assume that the velocity profiles depart from theory by a small but constant amount. Inside the sleeve of maximum velocity there is a regular pulsation of the vortex with a period of about one second, and this pulsation of intensity makes it difficult to "freeze" the anemometer with the stroboscope. The data points there actually represent the peaks of these surges in velocity, since it proved easier to measure the peaks than the lulls. It is not known whether the pulsation is due to the instrumentation or is a characteristic of the vortex, however

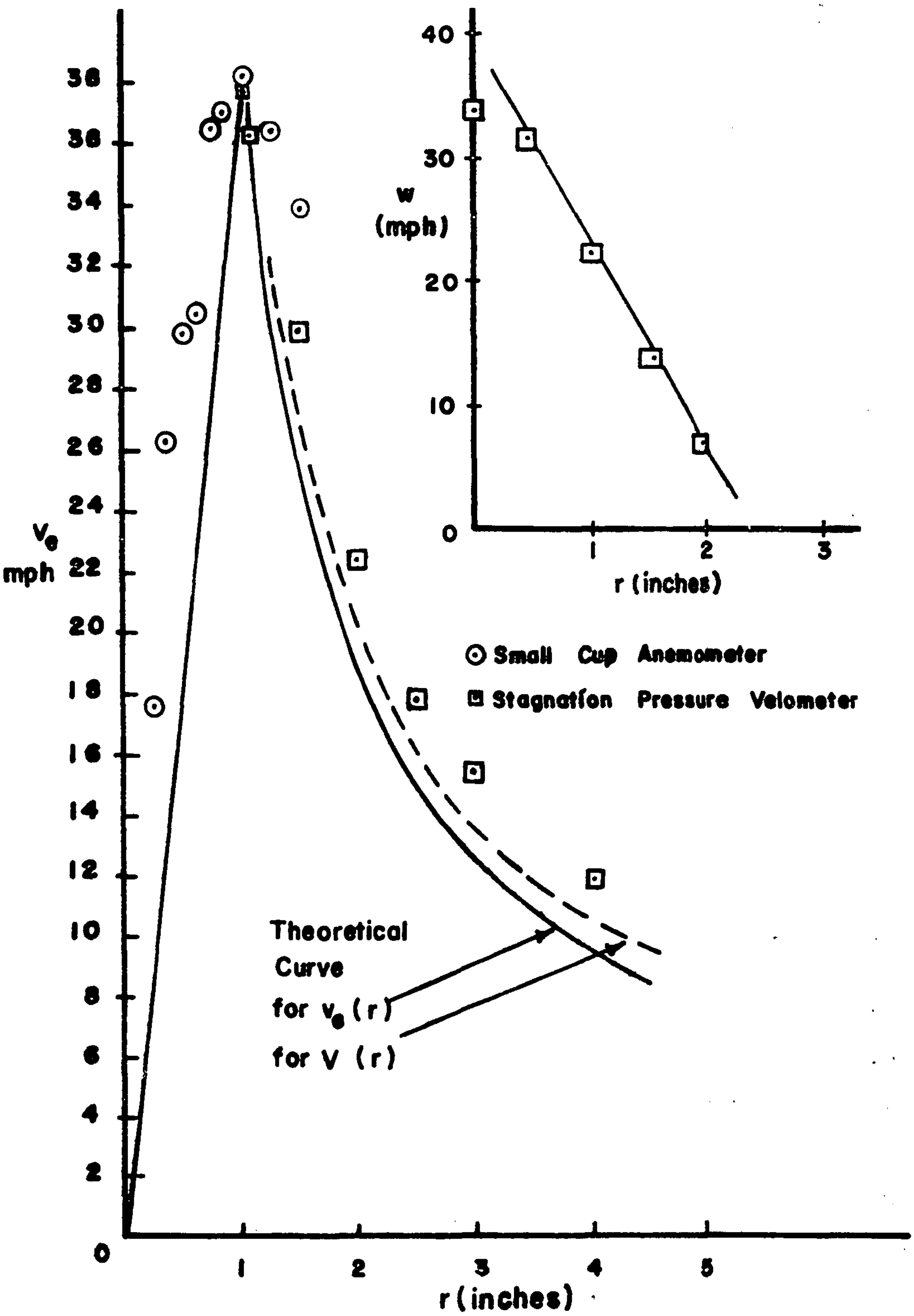

Fig. 7 Theoretical profiles of horizontal and vertical velocity with data points for the laboratory fast vortex.

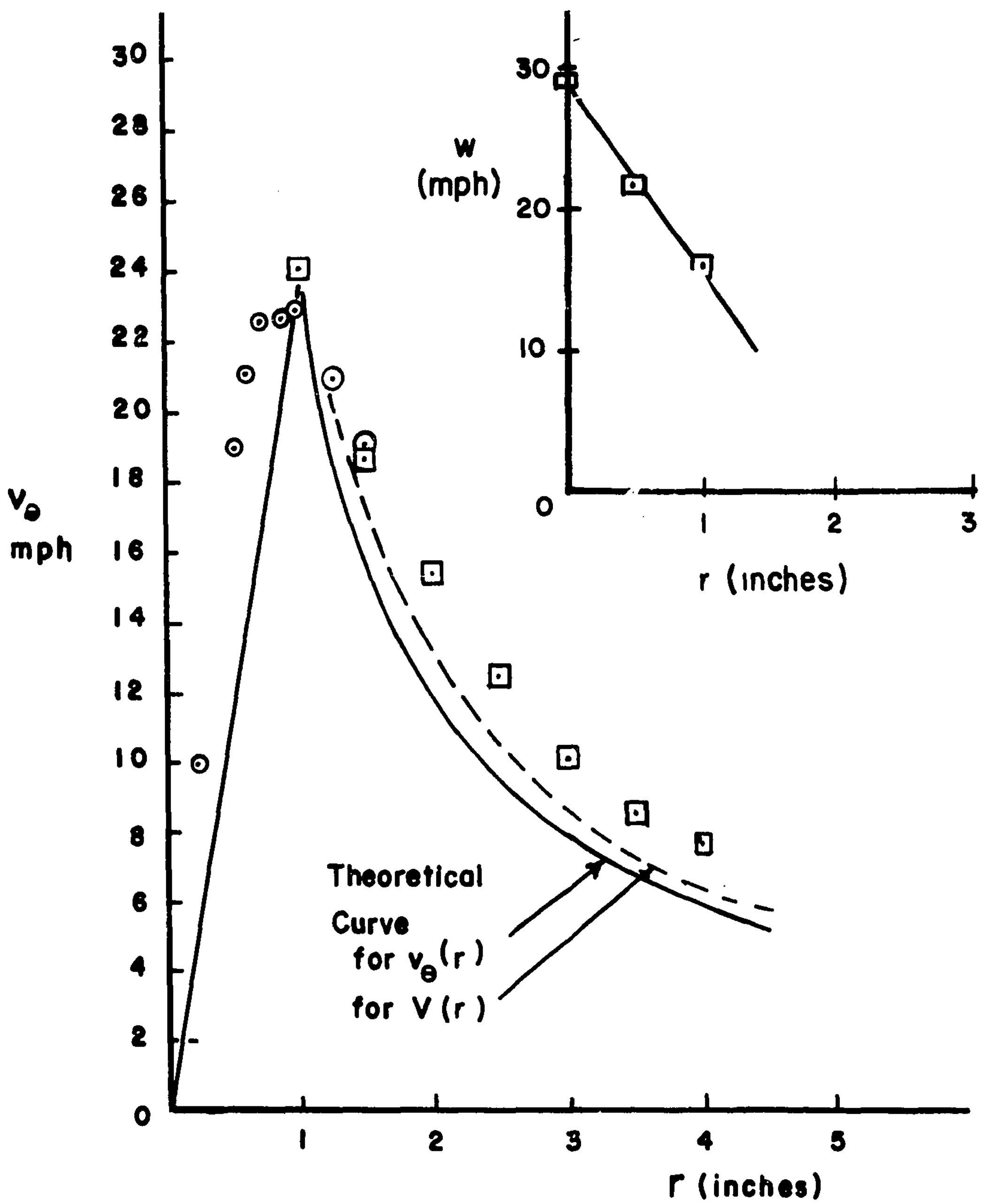

Fig. 8 Theoretical profiles of horizontal and vertical velocity with data points for the laboratory slow vortex.

other pulsation phenomena have been noted in the vortex, and these will be discussed later. The average velocity, if it were measurable, would show better agreement with the theoretical curve.

Recall that the motion equations for region I did not specify the profile of tangential velocity there. We noted earlier that this profile could be deduced from equation (11) if the distribution of vorticity is known. In particular equation (11) is satisfied by a function of the form

$$\zeta(r) = C\,(n+1)\,r^{n-1},$$

where C is a constant having the dimensions $T^{-1}\,L^{-n}$. In this case the velocity profile is

$$v_\theta(r) = Cr^n.$$

The constant C may be evaluated by taking n = 1 as

$$C = v_m r_m^{-n}.$$

The data points for v_θ in region I of Figure 7 are fitted approximately by taking n = 1/2, in which case

$$\zeta(r) = \frac{3}{2} v_m (r_m r)^{-\frac{1}{2}}, \text{ and } v_\theta(r) = v_m \left[\frac{r}{r_m}\right]^{\frac{1}{2}}.$$

This refinement is unnecessary for the problem at hand, but the method is applicable where data points in region I can be obtained with sufficient accuracy to assure that there is a considerable departure from the assumption of solid rotation. This refinement is only a second approximation, since it must be excluded from the vortex axis, where otherwise we would have infinite vorticity. On the other hand, there is no reason to object to the idea that the vorticity may become very large at small vortex radius, since this agrees with the observation (discussed in Chapter III) that the region I vortex grows vertically to boundaries quite rapidly, experiencing remarkably little decrease in intensity as it proceeds.

The radial profile of vertical velocity is approximately linear, as theoretically it should be, if the vortex sleeve is a conical surface, and if v_{rm} has a linear variation along the sleeve. Interestingly enough, the maximum rotation velocity is greater than the updraft velocity for the slow vortex, but not for the fast one, indicating that there is some optimum updraft velocity that will be most efficient in maximizing the vortex intensity.

The theoretical curves were derived from the equations of motion, particularized to the model vortex. The laboratory vortex has been shown to bear a reasonably close resemblance to the theoretical model. Further, the laboratory vortex is generated in such a manner as to bear the features generally attributed to the tornado, at least within the limitations of a laboratory modeling experiment of this kind. Henceforth we will use data from both model and laboratory vortex to assist in calculations that would be impossible without these tools.

Effects of Electrical Discharge Inside the Steady Vortex

Numerous documented observations of electrical discharges inside tornadoes has led Vonnegut [24] to question whether the association is purely fortuitous. Vonnegut was able to show that the electrical display cannot be caused by the vortex itself. Presumably there could be electrodynamic or thermal effects on the vortex, or both.

To investigate these effects, we will derive new motion equations with electrodynamic acceleration terms, and evaluate the magnitude of electrodynamic terms relative to aerodynamic terms. Then the thermal effect of a discharge will be discussed, and experimental evidence cited to assess its importance.

Motion Equation with Electrodynamic Accelerations

Let us suppose that a vortex region is rendered conducting by virtue of a concentration of ions resulting from electrical discharge. A current density j is defined by the motions of the ions, and a magnetic force B is present due to the current and also due to the geomagnetic field. The complete equation of motion is:

$$\frac{d\vec{V}}{dt} = \frac{1}{\rho} \nabla p - 2\Omega \times \vec{V} - \nu \nabla^2 \vec{V} + \frac{1}{\rho} (\vec{j} \times \vec{B}), \qquad (24)$$

where the latter term takes into account the Lorentz acceleration on the charged particles. If as before we resolve the vector acceleration components along cartesian coordinate axes, convert to cylindrical coordinates, neglect Coriolis and viscous terms, and assume steady-state motion and circular symmetry, we obtain the set

$$
\begin{aligned}
& v_r \frac{\partial v_r}{\partial r} + w \frac{\partial v_r}{\partial z} - \frac{v_\theta^2}{r} = -\frac{1}{\rho}\left[\frac{\partial p}{\partial r} - B_z j_\theta + B_\theta j_z\right] \\
& v_r \frac{\partial v_\theta}{\partial r} + w \frac{\partial v_\theta}{\partial z} + \frac{v_\theta v_r}{r} = \frac{1}{\rho}\left(B_r j_z - B_z j_r\right) \qquad (25) \\
& v_r \frac{\partial w}{\partial r} + w \frac{\partial w}{\partial z} = - g - \frac{1}{\rho}\left(\frac{\partial p}{\partial z} - B_\theta j_r + B_r j_\theta\right)
\end{aligned}
$$

This set of equations might be called the hydro-electrodynamic motion equations for a cylindrical vortex.

If a steady state is to exist we must require that B and j adjust to a situation in which the distribution of ion concentrations within the vortex remains constant. We might suppose that such a requirement could be met in a steady vortex having a continuous electrical discharge along its axis of rotation. We know that the vortex center is a preferred path for the discharge (see Vonnegut, Moore and Harris [28], and also Wilkins [31]).

In applying the new motion equations to our vortex model, we must inquire into the relative importance of the various electrodynamic terms. A tangential acceleration will derive from a combination of axial electric field and radial magnetic field, or from a combination of axial magnetic field and radial electric field. But we cannot conceive of any way whatsoever that a radial magnetic field can exist under the circumstances of our problem, so we reject the first of these situations immediately. This gives $B_r = 0$ in the above set of equations. Neither can a radial electric field have an important magnitude in the presence of the axial field maintaining the discharge. We see that a tangential electrodynamic force is very unlikely, but we will seek for other electrodynamic effects on the vortex. A small current density j_θ exists due to the rotation of charges in the vortex, giving rise to a very small component of B_z. This contribution to B_z is negligible compared with the geomagnetic component of B_z. B_θ results from the current density j_z directed along the vortex axis. A radial current j_r results if positive ions escape outward from the discharge column. It is the partial inhibition of this escape that makes the vortex axis a preferred path for the discharge.

Returning to the vortex model and resolving the motion equations into regions, we find in region I where $v_r = 0$,

$$\frac{v_\theta^2}{r} - \frac{1}{\rho}\frac{\partial p}{\partial r} = \frac{1}{\rho}(B_\theta j_z - B_z j_\theta)$$

$$\frac{\partial v_\theta}{\partial z} = -\frac{1}{\rho} B_z j_r \qquad (26)$$

$$0 = -g - \frac{1}{\rho}\frac{\partial p}{\partial z} - \frac{1}{\rho} B_\theta j_r,$$

and w is given by equation (14). In region II, where w = o,

$$v_r \frac{\partial v_r}{\partial r} - \frac{v_\theta^2}{r} = -\frac{1}{\rho}\frac{\partial p}{\partial r} - \frac{1}{\rho}(B_z j_\theta - B_\theta j_z)$$

$$\zeta v_r = -\frac{1}{\rho} B_z j_r \tag{27}$$

$$g + \frac{1}{\rho}\frac{\partial p}{\partial z} = \frac{1}{\rho} B_\theta j_r$$

The sets (26) and (27) represent the equations of the hydro-electrodynamic motions for our model vortex, further particularized to the condition of an electrical discharge along the vortex axis.

The conditions of our problem require that B_z be negative in the Northern Hemisphere, and that j_r be positive. B_θ is positive when j_z is positive (cyclonic sense when positive charges flow upward in the vortex center). This is consistent with a negative charge center in the thunderstorm cloud discharging through the vortex to the ground.

The most important contributor to tangential motion in the vortex, $B_z j_r$, occurs in the second equation of each set. In region I this term gives vortex intensity increasing with height. In region II the effect of this term should be entirely negligible, since the discharge occurs in region I. The possible magnitudes of the electrodynamic terms will be discussed later.

In the first of set (26) we see that $B_\theta j_z$ and $B_z j_\theta$ make a positive contribution to the cyclostrophic imbalance in region I, since B_z is negative. In other words, the centrifugal acceleration must balance both the pressure gradient and the electrodynamic accelerations. The discharge current, j_z, may be quite large. B_θ is the circular magnetic field resulting from the discharge current, and has the value

$$B_\theta = \frac{I}{2\pi\alpha r} \tag{28}$$

at distances from the vortex axis that are small compared with the length of the discharge. Here I is the discharge current (= j_z times cross section area of discharge) and α is the electromagnetic constant. Thus the electrodynamic term tends toward an increase in vortex intensity in region I if the pressure gradient remains constant. The magnitude of $B_z j_\theta$ would be most difficult to calculate, but must be very small compared with $B_\theta j_z$, since j_θ must be very small at any appreciable distance from the center of the discharge. $B_\theta j_z$ seems to be the most important electrodynamic force term.

The third equation in set (26) tells us that a departure from hydrostatic equilibrium results from an electrodynamic effect.

Region II is farther removed from the discharge, and the electrodynamic terms thus make much smaller contributions to the motion there. As we shall see later, the electrodynamic effect is also negligible in region I.

The Possible Magnitude of the Electrodynamic Effect

Returning to the contribution from the $B_\theta j_z$ force, we find that it must have the magnitude

$$B_{\Theta} j_z = \frac{I^2}{2\pi \alpha A r},$$

where A is the cross section area of the discharge. For a steady discharge, then, this electrodynamic term varies inversely with radius. In region I, where the discharge is assumed to occur, the centrifugal term must be proportional to r, owing to the velocity distribution in region I. This is shown by equation (12). If the flow were to remain cyclostrophic in this region then the pressure gradient would also vary directly with r. Therefore, the relative importance of the electrodynamic effect must decrease very rapidly with distance from the vortex axis.

The average lightning stroke carries a charge of about 20 Coulombs. If we assume that the "steady" discharge could carry charge at the same rate that occurs during successive lightning strokes in the same thunderstorm, then Jones' [12] observation of 20 strokes per second would give I = 400 amp. The diameter of the discharge is not known. While we call it a "steady" discharge, it is more likely to be a long series of discharges in rapid succession. According to Hagenguth [10], the maximum diameter of individual strokes probably is about 5 cm, giving $A \cong 20\ cm^2$. For density = 10^3 gm m^{-3}, we have

$$\frac{B_{\Theta} j_z}{\rho} \doteq \frac{0.125}{r}$$

in MKS units, or Newtons kg^{-1}. Multiplication by 100 converts to cgs units (10^5 dynes $Newton^{-1}/10^3 g\ kg^{-1}$), or dynes gm^{-1}.

We can set up a hypothetical situation for the purpose of comparing this term with that of the centrifugal acceleration. Let v_m = 10^4 cm sec^{-1} and $r_m = 10^4$cm, which is reasonable for a tornado. At a radius of one meter in the vortex the centrifugal acceleration would be 100 cm sec^{-2}, and the electrodynamic acceleration would be 0.125 cm sec^{-2}. This assesses the most important electrodynamic term. Since the electrodynamic acceleration is negligible in this calculation even very near the center of the vortex, and since it decreases with increasing radius (whereas the centrifugal and pressure gradient accelerations increase with radius in region I) we presume that a continuous electrical discharge in the core of a tornado will not make a significant contribution to vortex intensity as a result of electrodynamic effects.

Thermal Effect of the Discharge

We would expect then, that when an electrical discharge occurs inside of a tornado that the effect, if any, would be purely thermal in nature. Presumably the heat added by the discharge could provide additional buoyancy energy at vortex center, increasing the updraft velocity, adding to the radial inflow, and allowing the vortex intensity to increase by conserving the angular momentum of the additional inflow. On the other hand, the vortex must do work against the thermal expansion if it is not to increase in size. An increase in size would decrease the vortex intensity by angular momentum conservation, and confinement of the thermally expanding core would also require energy from the vortex.

The true nature of the electrical discharge sometimes seen in tornadoes is not known, and therefore the energy liberated can be only crudely estimated. The energy of the average cloud-to-ground lightning stroke is about 10^{17} ergs according to Schonland [23] and the stroke rate in a given region can be as high as 20 per second. This production of 2×10^{18} ergs sec^{-1} of energy must have an effect on a tornado if the energy is liberated along its axis. The question remains whether an increase or a decrease in tornado intensity will result.

One method for analyzing this effect is by assuming vortex contraction, or a change from one steady state to another as a result of work done by the additional buoyancy. This process is dealt with in Chapter III. Still another method is to compare steady-state vortices of the same size, one with the discharge inside, and one without. Since the motion equations cannot take into account the effect of a heat source along the vortex axis, we can best investigate this effect experimentally.

Experimental evaluation. The purpose of these experiments was to investigate the thermal effect of a continuous electrical discharge on a steady-state vortex. The vortex is the "fast" vortex described earlier, having a total pressure drop of about 36 mm H_2O and maximum tangential velocity of 38 mph. This vortex was shown earlier to correspond (as a scale model) to a 305 mph tornado. Fig. 9 shows this vortex "dyed" with $TiCl_4$ smoke.

The electrical discharge was powered by a 5 KVA transformer, connected through two choke coils to the 250 VAC outlet. The transformer and coils are shown in Fig. 10. Carbon electrodes were centered at the top and bottom of the vortex cage, and the top electrode could be raised and lowered to adjust the gap. The discharge is an AC carbon arc, and therefore may not be likened to the type that occurs in some tornadoes. Thus a similarity analysis for the discharge is not possible. Here the interest is limited to thermal effects, so that we need to know only the power available in the discharge. With electrodes separated 6 in the discharge current is 1.6 amp, and the potential across the electrodes is 800 V. The power is 1280 watts, or 1.28×10^{10} ergs sec^{-1}. This is to be compared for similarity purposes with the 2×10^{18} ergs sec^{-1} mentioned earlier as an estimate for the possible power for a discharge inside of a tornado.

For similarity purposes this power ratio should be compared with the ratio of the vertical flow rates in the model and in the tornado, since these represent volumes of air to be heated. We will assume this flow rate to be the product of updraft velocity and cross-section area of the sleeve of maximum tangential velocity. If the two vortices are exactly similar, we can use the velocity scale factor computed earlier,

Fig. 9. The laboratory fast vortex made visible by injection of $TiCl_4$ smoke.

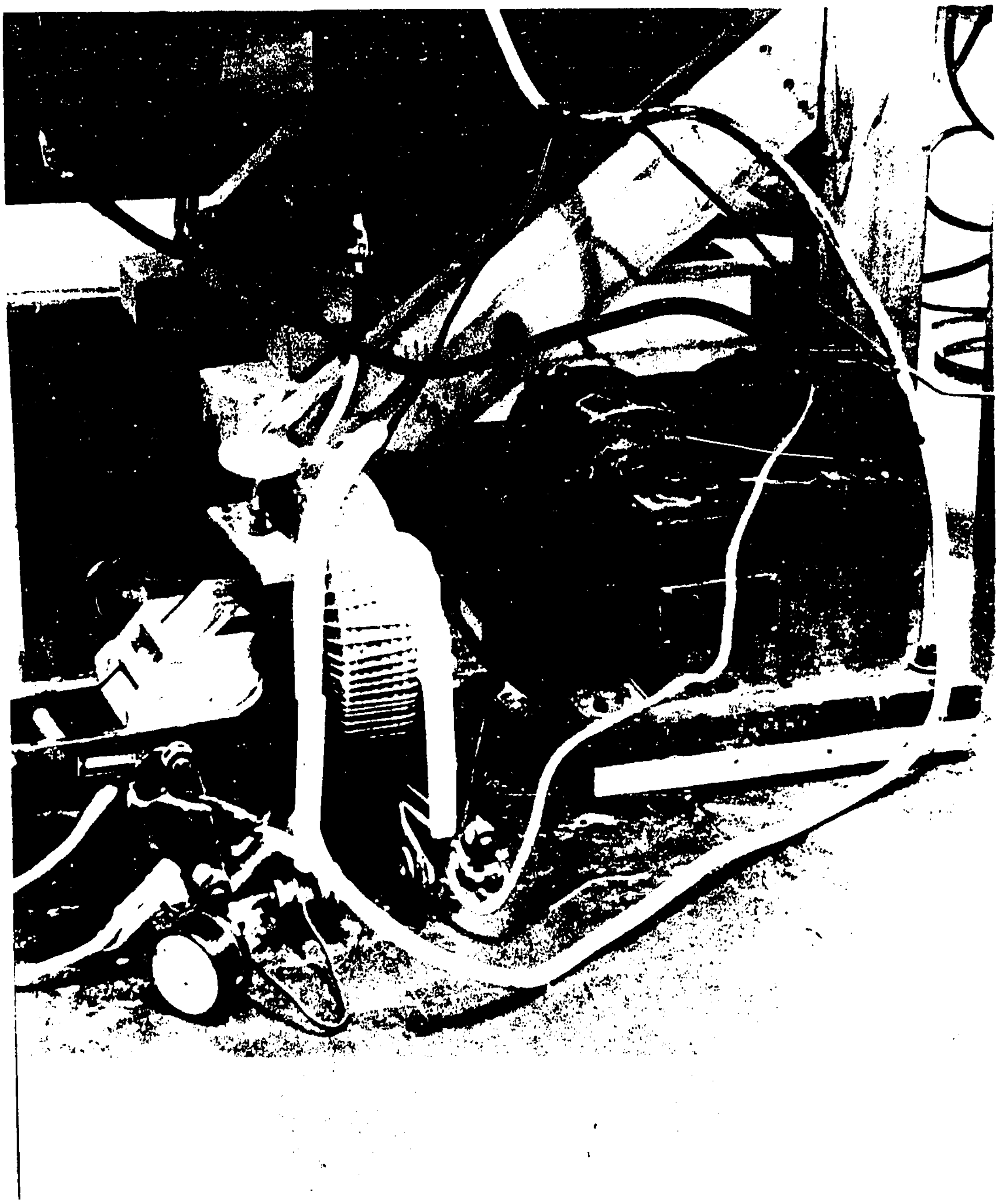

Fig. 10. Transformer and coils used to power the high-voltage AC arc.

which is 7.58. We use $r_m = 1$ in for the model, and $r_m = 100$ m for the tornado, and proceed with the similarity analysis as follows:

$$\frac{\text{Power (tornado)}}{\text{Power (model)}} = \frac{2 \times 10^{18}}{1.28 \times 10^{10}} = 1.56 \times 10^{8}$$

$$\frac{\text{Flow rate (tornado)}}{\text{Flow rate (model)}} = \frac{7.58\ \pi\ (10^{4})^{2}}{\pi\ (2.54)^{2}} = 1.18 \times 10^{8}.$$

These ratios agree closely enough for similarity purposes.

Figure 11 shows the discharge in still air, and Figure 12 shows the same discharge inside of the fast vortex. Comparison of these pictures indicates the degree of confinement of the plasma afforded by the vortex. Note that plasma streaks downward past the bottom electrode, indicating that the removal of heated air upward from the vortex center is not sufficient to offset the rate of thermal expansion taking place there. Indication of this fact is that the vortex total pressure drop decreases by 25 per cent, as indicated by the manometer at the center of the cage. No measureable downdraft occurs in this region of the vortex when the discharge is absent.

It was possible to measure the velocity profile to within 1 in of vortex center with the discharge present. There was no measurable change at a radius of 2 in or more. Figure 13 gives percentage decrease in vortex velocity between r = 1 in and r = 2 in. The decrease noted at the radius of maximum velocity is exactly that predicted on the basis of the 25 per cent decrease in vortex total pressure drop. For obvious reasons no attempt was made to measure velocities at smaller

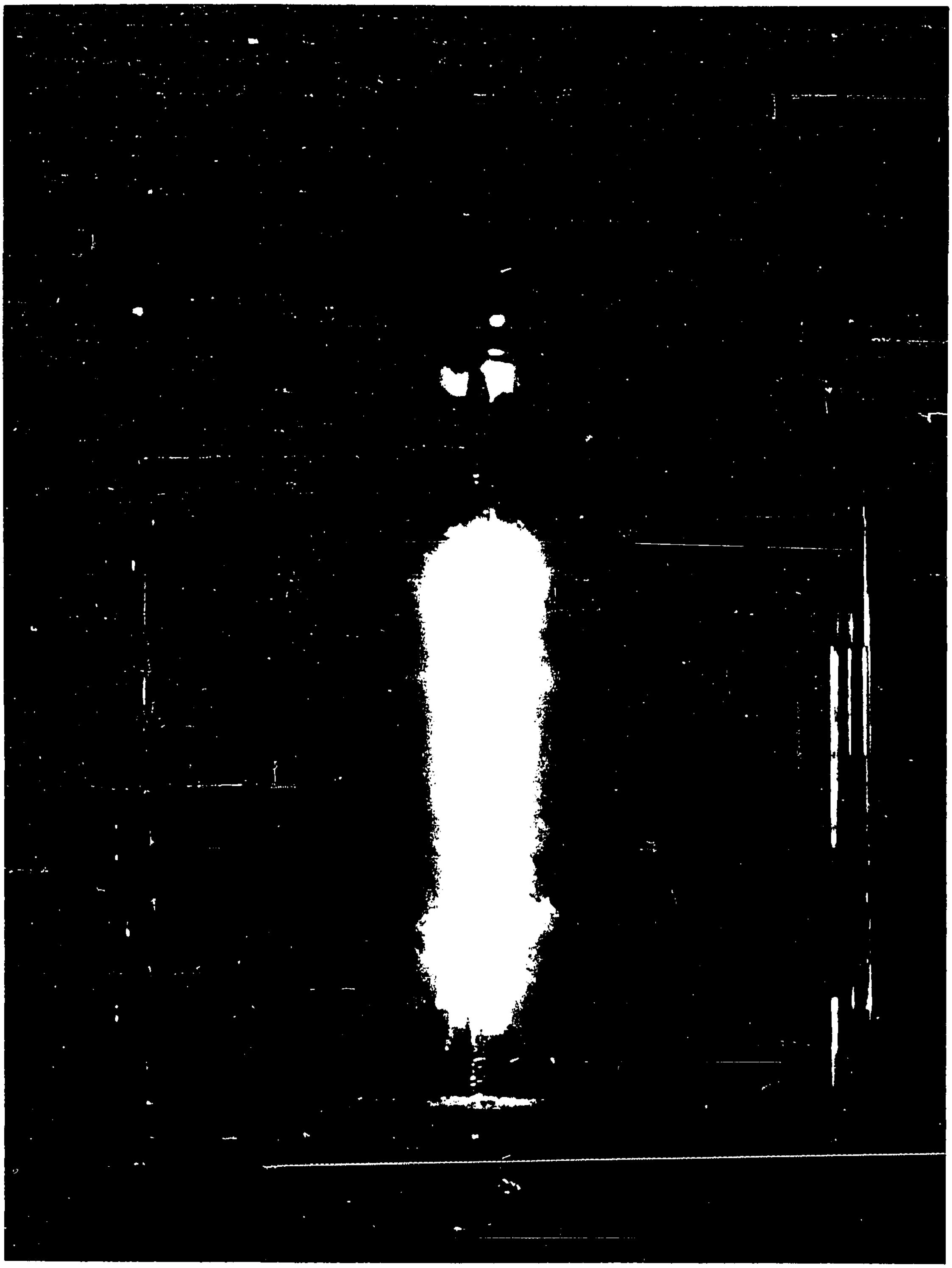

Fig. 11. The 1280-watt arc discharge in still air.

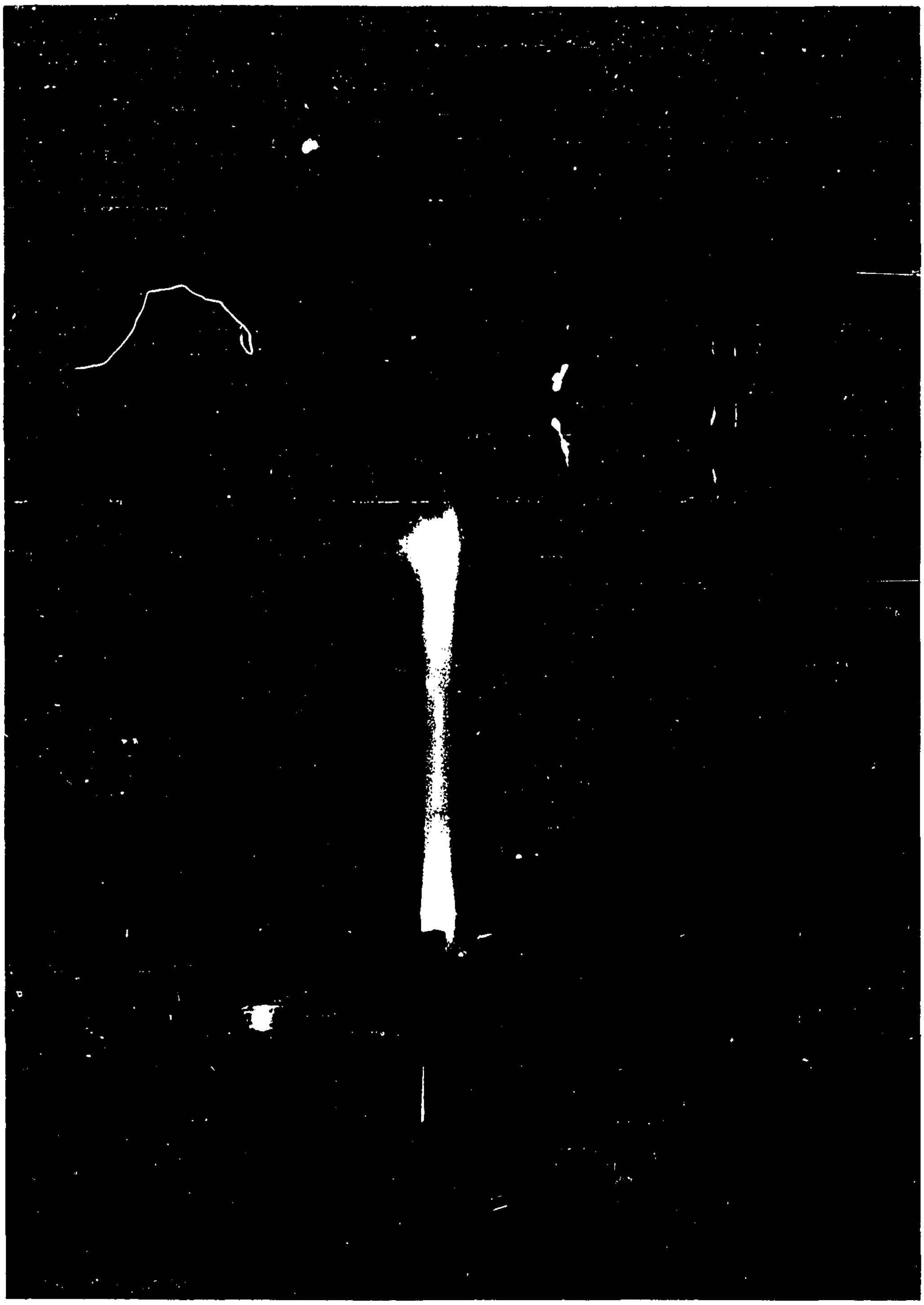

Fig. 12. The 1280-watt arc discharge in the fast vortex.

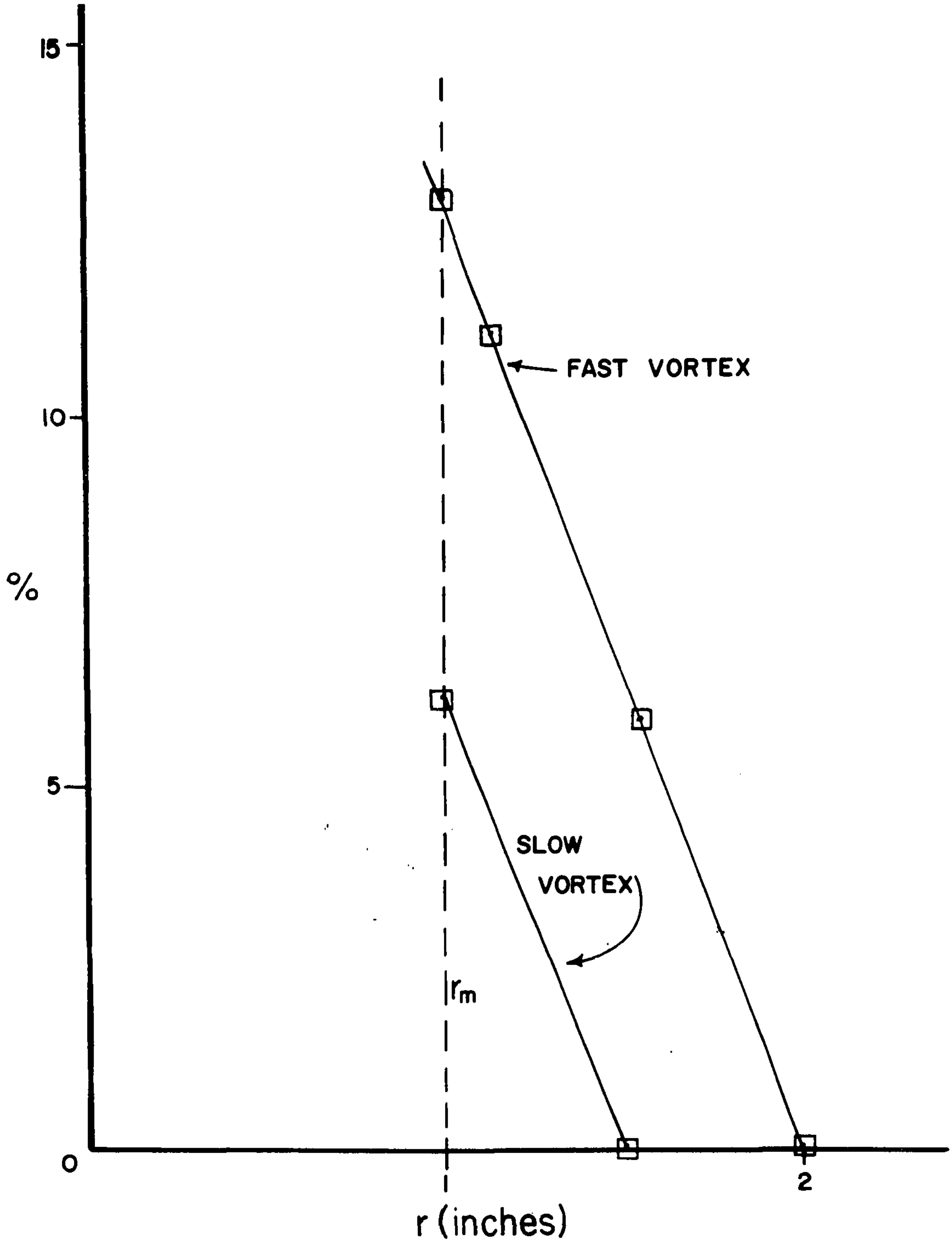

Fig. 13 Per cent decrease in $v_\theta(r)$ for discharge inside of vortex.

radii. Probably the new profile would be approximately linear between $r = 0$ and $r = r_m$, otherwise we would not likely have succeeded in verifying the new maximum vortex velocity by means of equation (20). It follows also that the 25 per cent decrease in pressure drop corresponds to a 25 per cent loss of kinetic energy in the vortex.

The same experiment was performed on the slow vortex with very similar results. The major difference appears to be that the plasma is only slightly less confined, as seen by comparing Figs. 12 and 14. Correspondingly, the slow vortex does less work on the plasma, and the decrease in vortex intensity is less, as shown in Fig. 13.

It is clear that vortex energy is used in confining the discharge gases, and therefore one would not expect a tornado to be more intense purely as a result of having an electrical discharge in its center. It seems rather more likely that the discharge would decrease the tornado's intensity.

There is an interest also in the vortex formed by the discharge itself. For this purpose the blower exhaust duct is removed from the top of the vortex cage, and the updraft is due solely to heat from the electrical discharge. Entrained air is given the same tangential component as before. The vortex thus formed is very slow and unsteady, and always whips the plasma away from the top electrode, as shown in Fig. 15. This, of course, extinguishes the discharge.

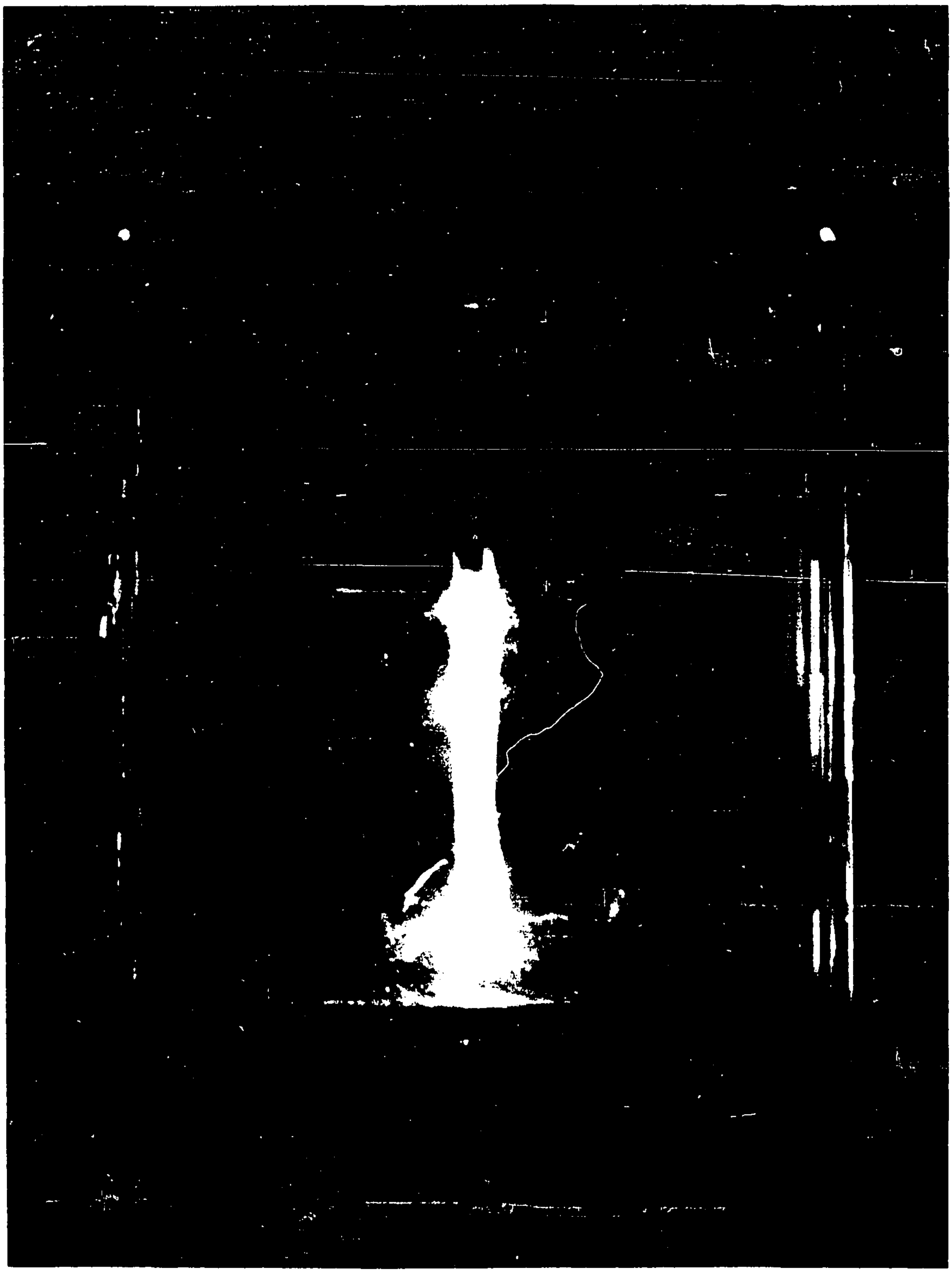

Fig. 14. The 1280-watt discharge in the slow vortex.

Fig. 15. Thermally-formed vortex.

Interest in the thermal vortex is due to the "fire whirlwind", which sometimes forms over large conflagrations, such as forest fires. Since well organized and sometimes very intense vortices form as a result of heat sources, we would like to determine whether the vortex formed by heat from the electrical discharge could also form a well-organized vortex. For this we need to prevent the plasma from breaking away from the top electrode until the vortex has time to become well formed. The breaking of the plasma may be inhibited to some extent by means of a "plasma shield", which is a perforated metal disc placed on the top electrode. The holes in the disc allow heated air to flow upward, while the larger electrode area represented by the disc retains better contact with the plasma as it meanders. Fig. 16 shows the discharge in a weak thermal vortex formed in this manner. The plasma is only poorly confined, and it is never possible to prevent the discharge from becoming extinguished prior to formation of a stable vortex, even with the plasma shield.

Miller [20] has shown experimentally that an organized vortex can be maintained by a heat source (non-electrical in this instance) after the vortex has been stabilized first by means of a blower. The present experiments verify Miller's result. Fig. 17 shows the discharge inside such a vortex. We share Miller's experience that the heat source finally had to be removed in order to prevent destruction of the vortex cage by the flame--this despite the fact that the top of the

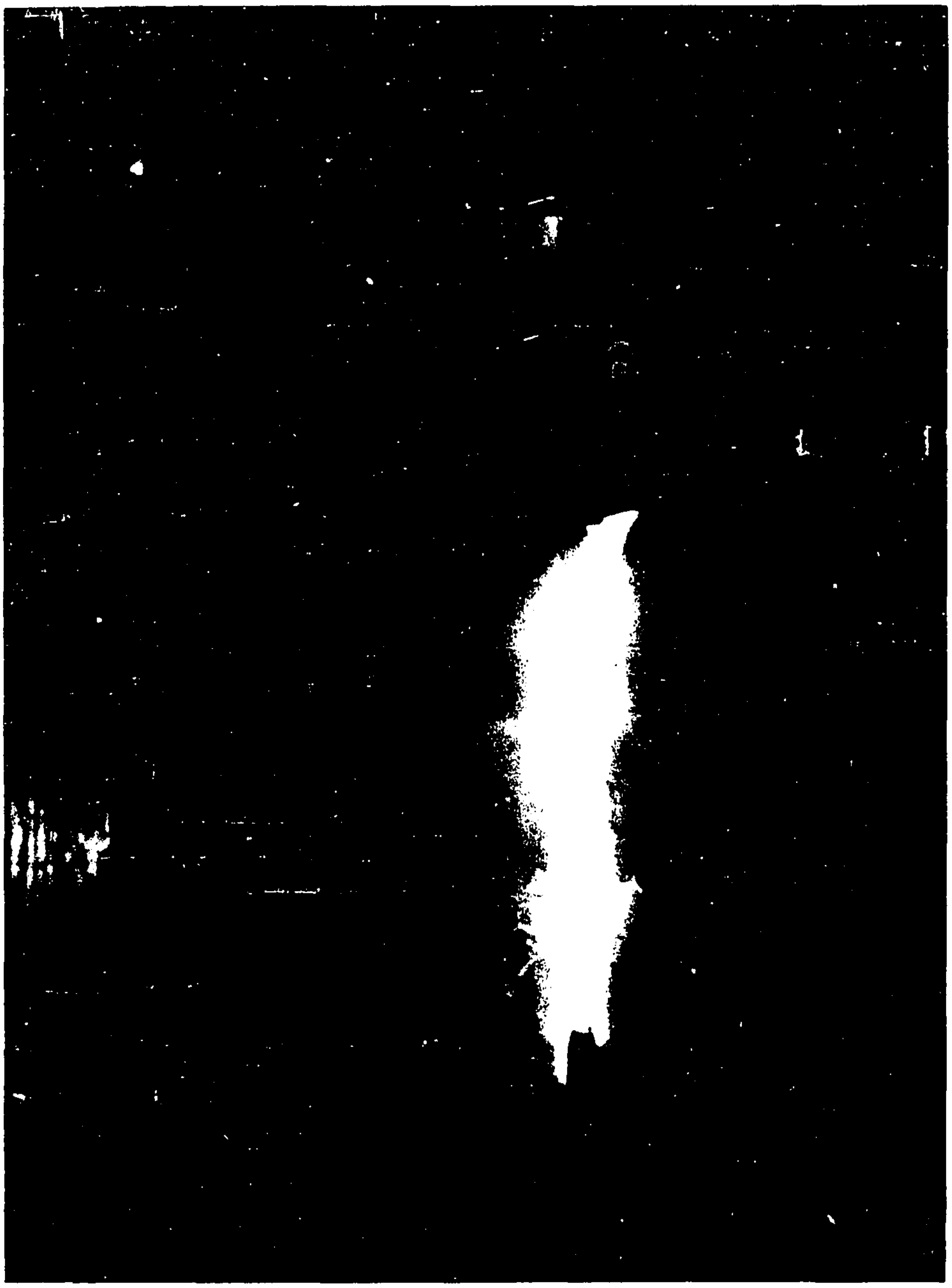

Fig. 16. Thermally-formed vortex with plasma shield on the upper electrode.

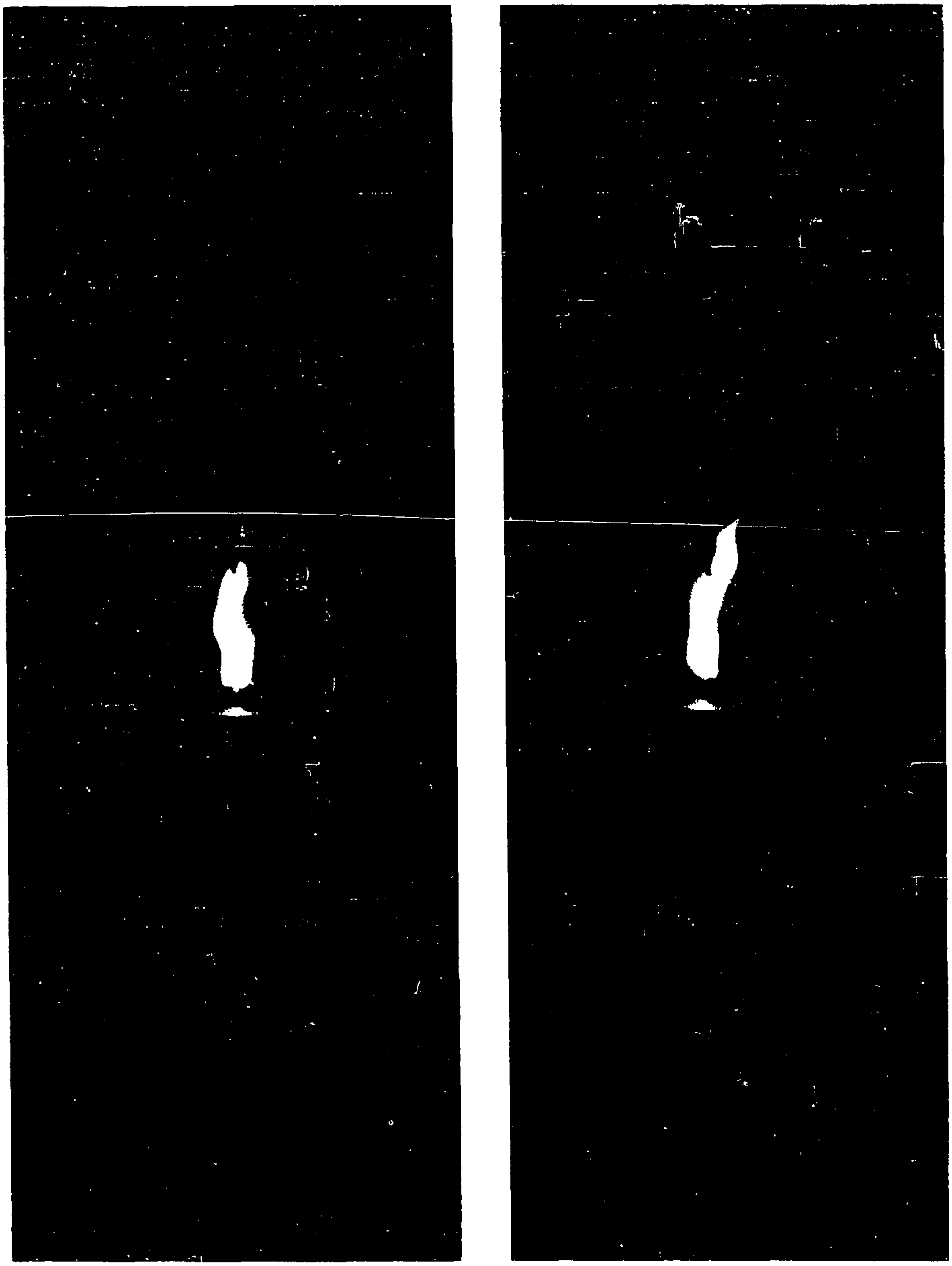

Fig. 17. Configurations of the plasma in the thermally-driven vortex, first stabilized by means of the blower intake.

cage was protected by 0.25 in sheet asbestos.

Fortunately it was possible to maintain the thermal vortex at least until it had time to reach a steady state. Even though the vertical transport of heat is much greater with the thermal vortex, the updraft and tangential velocities are immeasurably small, or less than 7 mph in this case. The reason for the greater heat transport without aid from the blower is that less cold air is entrained into the discharge, and thus the plasma is diluted less rapidly above the top electrode. Another factor is that the discharge current increases slightly when the discharge heat is allowed to come to equilibrium with its own updraft and entrainment.

This thermally-driven vortex is of interest also because the discharge inside of it is somewhat different in nature from that of discharges in still air, or even discharges in either fast or slow vortices that are driven by means of the blower intake. The plasma occupies a greater volume, and is not streaked by sputtering carbon particles. Thus it resembles more closely a glow discharge. The experiments of Vonnegut et al. [28] yielded changes from arc to glow-type discharge when the discharge environment was changed from still air to vortex. Since the thermally-driven vortex (first started with the blower) is the only one giving the glow-type discharge in the present experiments, and since Vonnegut used only a very weak blower in his experiments, we can suggest the following conclusions:

1) Vonnegut's vortex was actually thermally-driven rather than blower-driven, and the blower only served to give initial stabilization to the discharge.
2) If the discharge seen in a tornado resembles more closely the glow discharge, then possibly the vortex is powered largely by heat from the discharge, rather than from an external circulation system, even though a vortex may have been required initially in order to get the phenomenon started.

We have seen from this series of experiments that the thermal vortex owes its existence to a combination of rather ideal circumstances. We showed earlier that the energy of our laboratory discharge has model similarity to the maximum that could be expected from a thunderstorm. The optimum thermal vortex obtained with this discharge does not compare in intensity with that of the fast vortex, which was shown to bear model similarity to a tornado. We conclude that <u>thermal energy from lightning discharges alone is not likely to be directly responsible either for formation or for maintenance of tornadoes</u>. It does appear, however, that a vortex of intensity much less than tornadic could be maintained by heat from lightning discharges if the vortex were first created and stabilized by other means.

Chapter III

CHANGES OF STATE IN VORTICES

Up to now the analysis has been confined to the vortex in the steady state. In this section and in those to follow we will discuss conditions involving changes of state. While the steady-state vortex is difficult to treat mathematically, changes of state are even more complex. The motion equations tell us only that vortex intensity changes with time to accompany changes in the balance of forces in the vortex. Mechanisms for changing the balance of forces are not well understood, and we must rely on two rather qualitative methods for analysis of changes in state. One of these methods involves the observation of vortex formation and decay in the laboratory, where certain parameters may be measured and controlled. The other method calls for the analysis of changes from one steady state to another, where the change period itself is sufficiently brief that we may confine our attention to estimating only the energy required to bring it about, and to seeking for sources of such energy.

Tornado Formation

In Chapter II we saw that electrodynamic action cannot contribute significantly to the intensity of the steady vortex, and that the thermal release accompanying a vortex-centered discharge actually causes a decrease in intensity of the inner region of the vortex. One might reasonably expect that electrodynamic action would also be negligible in the formation of tornadoes. However, E. R. Rathbun [21] has hypothesized an "electromagnetic basis for the imitation of a tornado" which must be examined before this idea may be discarded entirely. The procedure here will be to show that Rathbun's basis for tornado formation is unworkable, and then to proceed with the analysis of other generative processes that are better supported by existing information on tornadoes and on vortex formation.

Formation by Electrodynamic Action (Rathbun theory)

Rathbun suggests that the steps leading to tornado formation are as follows:

(1) Negative charge accumulates in a cloud, increasing the electric field to the point of breakdown.

(2) A pilot leader stroke develops, but is not followed by a full stroke of lightning.

(3) A "considerable volume" of air is left ionized behind the pilot leader, which Rathbun assumes will contain 10^{10} or more positive ions per cm^3. This concentration of ions is supposed to last for "a number of seconds".

(4) The residual electric field, assumed to be 2 kv cm^{-1}, accelerates the ions upward, carrying along the surrounding air by ion-molecule collisions.

(5) A counterclockwise circulation (cyclonic vortex) derives from the tendency for the ions to spiral about a geomagnetic field line.

Rathbun goes on to calculate resultant air acceleration and vortex radius, using the data cited above. The objections that are fatal to this theory are as follows:

(1) Rathbun quotes Loeb [15] to justify the assumed concentration of ions behind by the pilot leader. Loeb's calculation is based on the assumption that a field of 30 kv cm^{-1} is required to initiate breakdown for a lightning stroke. More recent information, by Hagenguth [10] for example, shows that lightning strokes, owing to reduced pressure and high moisture content in the charge center's environment, may be initiated and completed in average potential gradients of about 100 volts cm^{-1}. We concede that the field may be non-uniform in the locale of the pilot leader's initiation. In the laboratory, 5 kv cm^{-1} would be sufficient to initiate breakdown, and in the vicinity of a thunderstorm cloud probably one tenth of this field would be sufficient. However, using the laboratory value of 5 kv cm^{-1} one may recalculate the ion concentration according to Loeb's method as about 10^9 cm^{-3}, which is an order of magnitude lower than the value used by Rathbun.

(2) The "considerable volume" of air ionized by the pilot streamer is also given by Loeb [15] but <u>not</u> quoted by Rathbun. It is a channel less than 0.5 cm in diameter and possibly several meters long. Rathbun computes a vortex diameter of about 3 m. Expansion of the column of ions to fill this volume would give further dilution of the ion concentration by a factor of 3.6×10^5.

(3) The least supportable assumption in the Rathbun theory is that the ions will remain in the pilot streamer channel for "a number of seconds". Apparently Rathbun has not understood the nature of sferics instrumentation, for he has assumed that the "long bursts" of sferics noise reported by Dickson [5] are somehow associated with the duration of ionization in the pilot leader of a single stroke. Actually the "long bursts" are due to several individual lightning discharges along a common azimuth within a period of one or two seconds. Individual strokes may be several kilometers apart. Rathbun has provided no evidence that the ions residual in the leader channel will be depleted at a rate less than that usually observed for discharges in air. Allowing Loeb's initial concentration of ions ($N_o = 10^{11} cm^{-3}$) along the pilot leader front and his method for estimating recombination, we write

$$\frac{N}{N_o} = \frac{1}{1 + N_o at}$$

where $a \doteq 2 \times 10^{-6}$ is the coefficient of recombination. We find that the ion concentration decreases to $5 \times 10^{6} cm^{-3}$ during the first second. The result of taking into account recombination gives an acceleration by the electric field of the air as a whole that is four orders of magnitude less than the 13.8 m sec^{-2} computed by Rathbun, and is indeed completely negligible.

The major objection to the Rathbun hypothesis is that ions will not be present in sufficient quantity for a long enough period to make it work. There are several additional objections, but these should suffice to dismiss the idea that tornadoes may be initiated by the acceleration of ions residual from lightning discharges. Since no better model than Rathbun's comes to mind for electrodynamic initiation of tornadoes, we feel justified in removing this kind of process from further consideration. In view of the weakness of the theory, an elaborate laboratory investigation of vortex formation by electrodynamic action is not warranted, however some preliminary experiments along this line were actually conducted, and are described later.

Formation by Vortex Contraction

For several years it has been conceded that a tornado could be formed by the sudden contraction of a larger vortex, say on the scale of a microcyclone, or "tornado cyclone". Conservation of angular momentum during the contraction would cause higher tangential velocities in the smaller vortex, or tornado. The microcyclone is sufficiently large that Coriolis force will assure counterclockwise rotation in agreement with observations on tornadoes. Yet the microcyclone is small enough to go undetected in the usual network of weather stations. If vortices of tornado size formed spontaneously outside of a microcyclone, then presumably either sense of rotation could be accommodated.

A well-documented and carefully-analyzed tornado situation has been presented recently by Fujita [8] which gives several instances of tornadoes forming near the center of a microcyclone. The microcyclone itself apparently forms due to convergence of air into a larger region of convection. In the cases analyzed by Fujita the microcyclone moved along, occasionally producing a tornado near its center. This suggests a sudden jet-like updraft, small in diameter compared with the microcyclone, and occurring somewhere inside the microcyclone. We would suppose that the most likely source of buoyancy for the updraft is the release of the latent heat of condensation, or perhaps heating of the air by lightning strokes occurring in rapid succession. These possibilities will be discussed further later.

The Vertical Growth of Incipient Vortices

In region II air spirals radially inward and in region I air spirals vertically upward. The region I vortex grows upward as far as the up-draft and the tangential velocity component in the updraft will reach--experimentally the upper boundary is the top of the vortex cage. In the free atmosphere presumably, the upper boundary may be due to a stable layer. Viscous forces are negligible compared with the other vortex forces, so that the region I vortex may extend itself a considerable distance from region II.

A series of experiments was performed with the vortex cage to determine what would be the differences in the nature of the vortex if air was allowed to be entrained tangentially through a narrow slot at the top, bottom, or center of the vortex cage. These cases were also compared with the one in which tangential entrainment occurs throughout the entire depth of the cage. It turned out that there was essentially no difference at all in these vortices. By the time the steady state was reached (almost instantly in all cases), the pressure drop and maximum velocity was the same. Since air is exhausted from the top of the vortex cage, it is rather difficult to see how the vortex grows instantly to the bottom of the cage, even when the entrainment is restricted to a narrow slot at the top. The fact that the pressure drop for this case is the same as for the others is evidence enough that the vortex does indeed grow to the bottom of the cage, since the manometer opening is located there. We are discussing here the optimum or fast vortex with $K = 0.36$, $\Delta p = 3.6$ cm H_20 and $v_m = 38$ mph.

The implication of these experiments is clear that the type of vortex under consideration may be created and maintained by a narrow layer or jet of air directed tangentially into a region of updraft, and further that the vortex so formed will grow vertically to the boundaries. It appears also that neither the probability of vortex formation nor the pressure and velocity distribution of the vortex when it reaches the steady state will be particularly sensitive to the elevation of the jet relative to the updraft, as long as the K-factor is sufficiently optimized.

Vorticity Induction Experiments

We have already seen how the vortex cage may be used to generate "scale-model" tornadoes by entrainment of a tangential component due to the air entry vanes of the cage. If we remove the tangential component at the sides of the cage, we can attempt to induce vorticity into the updraft in the cage by other means. The method used was to create wind shears with a fan and blower external to the cage, and to observe the effect when these shears were entrained into the updraft. The results were entirely negative, for no vortex could be generated in this manner.

The original plans for this program also called for experiments to induce vorticity by means of electrodynamic accelerations. The idea was to provide a supply of ions by means of point discharges, accelerate them with an applied electric field, and cause vortex motion by deflecting the ions with an external magnetic field. Theoretically such a vortex would be possible under ideal circumstances (see Lewellen[14], for example) but <u>not</u> under the conditions to be found in thunderstorms. Preceding analyses in this paper have shown that electrodynamic accelerations cannot be important in tornado formation or maintenance. Some experiments of this kind were conducted with apparatus described in an earlier report[31], but with negative results. This kind of experimentation was abandoned when it was found not to be appropriate for tornado research. Construction of apparatus actually capable of producing electrodynamic vortices is inappropriate to this program, since no similarity to tornado processes could be demonstrated with such equipment.

The necessary and sufficient laboratory conditions for creating and maintaining a vortex bearing a scale similarity to a tornado were described in the preceding section. No other methods attempted have succeeded in producing a vortex of this type. Whether it is possible to create such an atmospheric vortex by other methods has yet to be demonstrated.

Energy Requirements for Vortex Contraction

In the laboratory vortex it is observed that the optimum K-factor is constant over a wide range of updraft velocities. Therefore an increase in updraft velocity w, which causes an increase in radial velocity v_r, will also be accompanied by a corresponding and proportional increase in v_Θ, or vortex intensity, from the conservation of angular momentum.

Now in the free atmosphere vortex a sudden increase in w must also cause an increase in v_r and v_Θ. If v_Θ does not increase with v_r, then angular momentum conservation contributes nothing to vortex intensity, which means simply that air is being fed into the vortex without a tangential component. In the laboratory this has the effect of destroying the vortex instantly, even if the air fed in nontangentially enters from only a very small zone of the vortex cage. We deduce that the air must be fed tangentially to the vortex in an organized fashion in at least one shallow layer somewhere between the top and bottom of region I and must be restricted from entering elsewhere. This organized tangential component is the air entry vane in the vortex cage, and in the case of the tornado it must be the parent microcyclone. The laboratory vortex intensifies "in place" when w is increased, whereas in the free atmosphere the microcyclone is subject to no mechanical constraints, and thus may "collapse" to form a more concentrated vortex. Of course, the air moving in to replace the collapsing microcyclone moves on a scale sufficient to be subject to Coriolis force, and may form a new microcyclone. Thus the microcyclone need not vanish as a result of the contraction. Brooks' [4] scheme for tornado formation embodies the principle of the contracting microcyclone, and Fujita's [8] observations show that the microcyclone need not disappear when a tornado forms.

With these thoughts in mind we will now use the vortex model to analyze the effects of vortex contraction and the order of magnitude of energy required. Just as before, we will analyze the situation in terms of two separate vortices, or regions. A vortex region in solid rotation lies concentrically within a vortex region in irrotational motion. If we confine our interest to changes that will take place in the profile of tangential velocity as a result of vortex contraction, we can make use of our earlier results. We recall that the model was derived for the steady state, and so we will assume that we have a steady state initially and also immediately following the sudden contraction. This simplifies the problem essentially to that of investigating what happens at the radius of maximum tangential velocity, since we will require that region I remain in solid rotation after contraction, and that region II remain irrotational. The logic behind this requirement is as follows:

1) Solid rotation in region I was considered possible because of the fact that vertical motion predominates over radial inflow there. The role of region I is to exhaust vertically the air brought in by convergence. During contraction region I still plays the same role. We say, then, that no

component of radial velocity occurs <u>inside</u> of region I during contraction, but rather that region I retreats inward just in advance of the contraction.

2) Irrotational motion derived in region II as a result of the requirement that the tangential velocity profile there remain constant (steady-state) in spite of the angular momentum conservation associated with radial inflow. In a sense, then, region II is undergoing contraction even in the steady state. We would expect that the profile of tangential velocity there would retain its shape during contraction, even though the magnitude of the tangential velocity changes.

Denote with subscripts 1 and 2 the values of radius and velocity before and after contraction respectively. Conservation of angular momentum requires that

$$v_{m2}\, r_{m2} = v_{m1}\, r_{m1}. \qquad (30)$$

We see that the maximum tangential velocity is increased by the factor $\frac{r_{m1}}{r_{m2}}$. A factor of five decrease in radius of region I gives a five-fold increase in the maximum tangential velocity, and the resulting change in velocity profile is shown in Fig. 18. It seems clear from this that vortex contraction is a mechanism whereby tornadic velocities may be realized in this model. Following contraction, the energy required for vortex maintenance need be no greater than required to overcome the relatively small viscous forces.

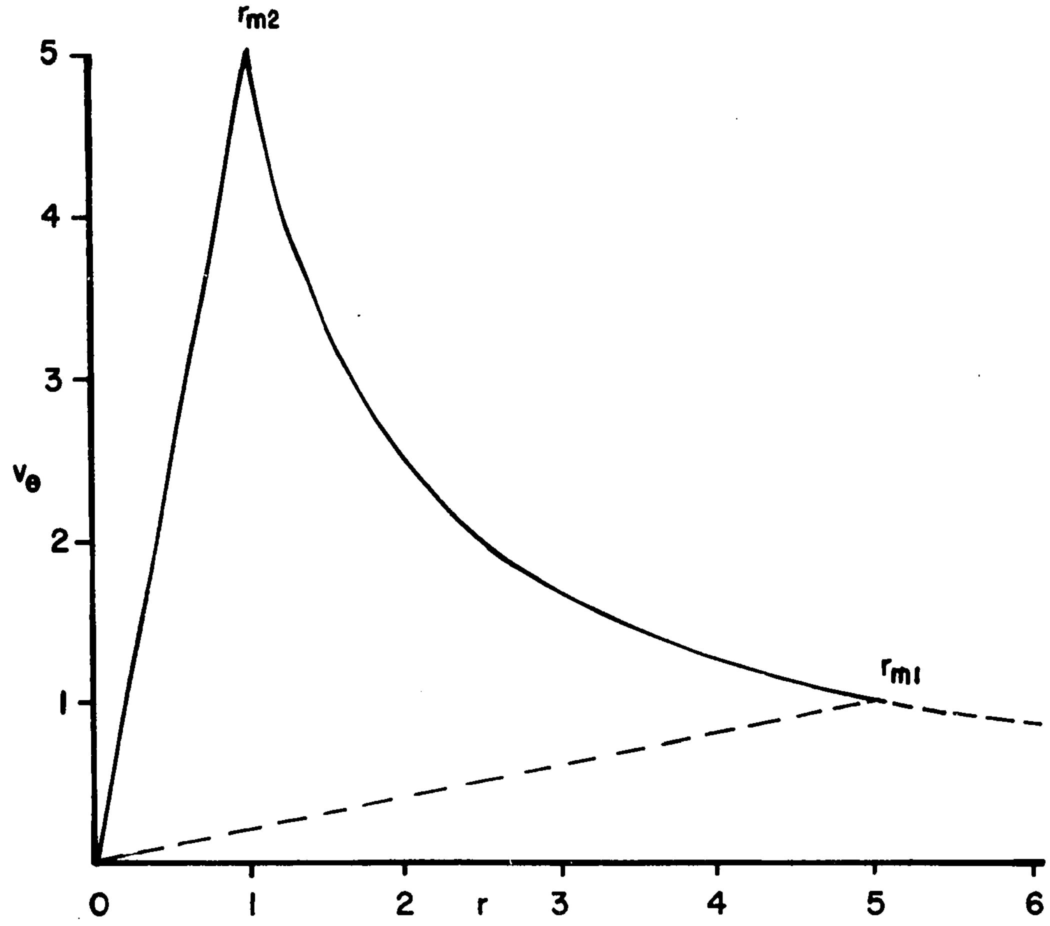

Fig. 18 Effect of contraction of the model vortex on the profile of tangential velocity component. r and v_θ are in arbitrary units.

The velocity profiles of the model vortex also give the distribution of kinetic energy, and integrations can be performed to obtain the increase in kinetic energy due to contraction. This change in kinetic energy can be related to the energy derivable from buoyancy forces, which presumably gives rise to such a contraction in the first place. Such calculations have been carried out by Fulks[9], but not correctly, since he considered only the kinetic energy in region I of the vortex.

The kinetic energy per unit mass of a horizontal slice through the vortex is

$$KE_I = \frac{1}{2}\left(0 + \frac{v_m^2}{2}\right) = \frac{v_m^2}{4} \qquad (31)$$

in region I, since the velocity profile is linear there, and the integrated energy profile is simply the average for the region. In region II the kinetic energy is

$$KE_{II} = \int_{r_m}^{r_o} \frac{V^2}{2} \cdot \rho \cdot \Delta h \cdot 2\pi r dr.$$

The specific volume of the slice is $\pi(r_o^2 - r_m^2)\Delta h$, where r_o is some arbitrary radius at which V can be presumed negligibly small. Recalling that $V^2 = v_{II}^2 + v_r^2$ in region II; and that $v_{II} = \frac{v_m r_m}{r}$, $v_r = \frac{v_{rm} r_m}{r}$, we may write

$$KE_{II} \doteq r_m^2 \frac{(v_m^2 + v_{rm}^2)}{r_o^2 - r_m^2} \int_{r_m}^{r_o} \frac{dr}{r} \qquad (32)$$

for the kinetic energy per unit mass in region II. The total kinetic energy per unit mass for the horizontal motion is

$$KE_I + KE_{II} = \frac{v_m^2}{4} + r^2{}_m \left(\frac{v_m^2 + v_{rm}^2}{r_o^2 - r_m^2} \right) \ln \frac{r_o}{r_m} . \qquad (33)$$

The kinetic energy per unit mass in region II depends on the K-factor, but is not negligible, even when the K-factor itself is very small.

Consistent with Fulks' earlier assumptions (ibid., p. 21) about his model, we take $r_o = 2.5\ r_m$, and using K = 0.36, as found optimum for the laboratory vortex, we can reduce equation (33) to

$$KE_I + KE_{II} = 0.25\ v_m^2 + \frac{1.13 v_m^2}{5.25}\ (0.916)$$

$$= 0.25\ v_m^2 + 0.2\ v_m^2 = 0.45\ v_m^2 . \qquad (34)$$

This shows why the kinetic energy in region II may not be neglected. Actually we cannot be sure that K = 0.36 is also optimum for a tornado. "Optimum" here means obtaining the maximum tangential velocity for a given range of updraft velocities. This value of K will suffice until better ones can be measured. Anyway, the kinetic energy in region II is not at all sensitive to the value of the K-factor. To continue the calculation,

Work done on vortex = mass x 0.45 ($v_{m2}^2 - v_{m1}^2$) ; (35)

where the mass is $\pi(2.5r_{m1})^2h\bar{\rho}$, and h is the height of the vortex.

Energy from Buoyancy Forces :

An estimate of the rate of work available from buoyancy forces to contract the vortex is given by

$$\frac{dW}{dt} \doteq \frac{\pi r_{m1}^2}{2} h\bar{\rho}\, wg \frac{\Delta T}{T}, \qquad (36)$$

where $g\,\Delta T/T$ is the average buoyancy acceleration, and w is the average increased vertical velocity during contraction. The factor of 1/2 is due to the assumption that only one half of the energy of buoyancy is effective in contracting the vortex. We can multiply by the period Δt during which contraction takes place, and then equate the work available from buoyancy forces to that required to contract the vortex. This gives the relation

$$v_{m2}^2 - v_{m1}^2 = .178\, wg \frac{\Delta T}{T} \Delta t, \qquad (37)$$

from which the increase in maximum tangential velocity is obtainable. Using the following substitutions (after Fulks) w = 20 m sec^{-1}, Δt = 10 min., average $\Delta T/T = .01$, and v_{m1} = 20 m sec^{-1}, we calculate that v_{m2} = 24.7 m sec^{-1}, as compared with 53 m sec^{-1} computed by Fulks by neglecting the kinetic energy in region II. Even if all the buoyancy force were available for vortex contraction v_{m2} would be only 28.6 m sec^{-1}. It appears reasonably certain that this amount of buoyancy force alone will not give rise to the contraction and thus to the highly concentrated zone of kinetic energy which is the tornado vortex.

The only alternative is that the seemingly reasonable value of buoyancy calculated by Fulks is sometimes greatly exceeded locally in severe thunderstorms, say by a factor of 50, if a 100 m sec^{-1} vortex is to be obtained. This would seem to imply that only the giant convective storms could supply the buoyancy required to form a tornado by vortex contraction.

Recent Data on Available Buoyancy

We assumed earlier that probably only one half the energy available from buoyancy forces would be utilized in contracting the vortex. It is reasonable to assume that the other half would be utilized in overcoming resistance, or negative energy, as required when giant convective storms penetrate deeply into stable layers, such as the stratosphere. With this assumption, we may then equate the energy calculated from an observed penetration of the stratosphere to the amount of energy usable for vortex contraction, and thus utilize information available from recent observations on severe convective storms.

Donaldson et al. [6] have published radar data obtained during a tornado-producing storm that occurred in July, 1958. Radar echoes penetrated 13,000 ft into the stratosphere to occupy a volume there of 800 km^3. The penetration energy is computed on a thermodynamic chart to be 1.7×10^{21} ergs. Time lapsed between the observation that the storm was developing and the time that it had penetrated 13,000 ft into the stratosphere was only 29 minutes, corresponding to a rate of about 10^{18} ergs sec^{-1}. This is 100 times greater than the energy rate that Fulks assumed to be available from buoyancy forces. We required only a factor of 50 increase in work available from buoyancy forces to obtain a 100 m sec^{-1} vortex formed by contraction. The mystery as to whether the energy was available from buoyancy forces has now been resolved affirmatively, but the problem now becomes one of determining the mechanism by which this force attains so great a magnitude.

Still another approach to the calculation of buoyancy force may be based upon an observation reported by Beckwith [2], that four-inch diameter hailstones occurred (and were encountered by an aircraft) at an elevation of 40,000 ft. This elevation was very near the tropopause, and we can compute the updraft velocity required to support a hailstone of this size, and then estimate the penetration energy and depth for a standard stratosphere.

In calculating the supporting updraft velocity we solve for the hailstone's terminal velocity, which is defined when the drag force is balanced by gravity. Using data published by Mason [19], assuming a hailstone density of 0.4 gm cm^{-3} and an air density appropriate to

40,000 ft, we calculate the sustaining updraft velocity to be 80 m sec^{-1}. The Vonnegut and Moore [26] rule says that this velocity corresponds to a stratosphere penetration of 4 km by a thunderstorm (one km for each 20 m sec^{-1} at the tropopause) and the energy required is about 1.5×10^6 erg gm^{-1} of air for a standard stratosphere. The 4 km (13,000 ft) of penetration into the stratosphere is the same as the penetration cited earlier for the storm observed by Donaldson et al. We may then regard this as supporting evidence that buoyancy forces do occur with more than sufficient energy to contract a microcyclone into a tornado. In a convectively unstable atmosphere an updraft, once initiated, will continue to accelerate due to releases of latent heat. The calculation of this acceleration for a realistic model is a rather difficult problem in condensation phenomena, the solution to which has not yet been found, and which is entirely beyond the scope of this investigation.

Heating by Lightning Discharges

Vonnegut [24] has suggested that additional buoyancy could be supplied in the center of a vortex by the heat from lightning discharges. The energy of the average cloud-to-ground lightning stroke is on the order of 10^{17} ergs. At a stroke rate of 20 per sec some 2×10^{18} ergs sec^{-1} may be transferred to the air in the form of heat, if these strokes occurring in rapid succession have average energy. This is the equivalent of 4.16×10^{10} gm cal. At one atmosphere and 20C the specific volume is 0.024 m^3 (gm mole)$^{-1}$. Using a specific heat of 7 gm cal (gm mole°C)$^{-1}$, we see that 291 gm cal are required to raise each cubic meter of air one degree C. Then 10^4 gm cal m^{-3} will be required to attain $\Delta T = 42C$, which when combined with $w = 80$ m sec^{-1} would give the buoyancy force required to contract the microcyclone into a tornado according to the conditions prescribed earlier, provided that the volume of air affected is sufficient to contract the vortex.

The volume of air that can be heated to the necessary temperature by the lightning is

$$\frac{4.16 \times 10^{10} \text{gm cal}}{10^4 \text{gm cal m}^{-3}} = 4.16 \times 10^6 \text{m}^3.$$

A column of air 1 km tall so heated would have a diameter of only 71 m, whereas the volume change resulting from the vortex shrinkage required for a 100 m sec^{-1} tornado (from our model with r_{m1} = 500 m to r_{m2} = 100 m and v_{m1} = 20 m sec^{-1}) is represented by a cylinder of 245 m diameter. The heating by lightning is too small to accommodate this model by a factor of more than 10^4. Stated differently, the volume change due to displacement of air heated by lightning is only sufficient to give the required five-fold increase in vortex intensity when the volume change is

$$\pi 10^3 (r_{m1}{}^2 - r_{m2}{}^2) = 4.16 \times 10^6 \text{m}^3,$$

for a vortex 1 km tall. Substituting $r_{m1} = 5r_{m2}$ gives r_{m2} = 7.5 m, and thus r_{m1} = 37.5 m.

One could argue that the contraction of a vortex of 75 m diameter into one of 15 m diameter to achieve tornadic velocities is not at all unreasonable. The larger vortex, having a maximum tangential velocity of only 20 m sec^{-1}, could easily go unnoticed in the observational network, whereas the smaller vortex with v_m = 100 m sec^{-1} would be most destructive. Even though the heating by lightning has been purposely maximized in this simple calculation, the calculation suffices to place heating by lightning within the realm of possible contributory mechanisms. This is true even though the work derivable from buoyancy in the case of lightning heating is four orders of magnitude smaller than that observed from thunderstorms penetrating the stratosphere.

We must recall, however, that the tornado is observed to be in the dissipation stage when its diameter decreases to such a small value that it has a rope-like appearance. Furthermore, if sufficient buoyancy were released by lightning heating to contract a vortex from 1000 m to 200 m in diameter, the discharges would have to continue for several minutes. If this were an important mechanism for tornado formation, then we would expect a much higher correlation between tornado formation and sferics than that reported by Jones [12]. It is possible, however, that heat from lightning may in some cases initiate a strong updraft, which subsequently becomes accelerated as a result of convective instability.

Tornado Dissipation

Tornadoes are observed to dissipate either by withdrawing upward or by going through the "rope" stage. Now let us suppose that region II of the tornado vortex is confined to a layer aloft, and that the region I vortex has grown downward to the ground as would be expected from the laboratory experiments cited earlier. With this situation the tornado would withdraw upward if the updraft were gradually interrupted. Furthermore, the tendency for some tornadoes to skip about from place to place could be explained as temporary interruptions of the convective updraft. Occurrence of convection in bursts is the rule rather than the exception.

The tornadoes analyzed by Fujita[8] dissipated by going through a stage in which the vortices became long and narrow, with their axes almost horizontal over much of their length. In each case the tornado had moved out from under the parent microcyclone when it dissipated, and so the rope-like, leaning vortex appears to be associated somehow with asymmetry of the vortex axis with respect to the organized pattern of the tangentially directed inflow upon which the vortex feeds. That such an asymmetry would result in weakening the vortex is not surprising but the reason for the rope-like appearance is not explained. However, this phenomenon is easily duplicated in the laboratory.

Laboratory Experiments with Decaying Vortices

Vortices formed in the vortex cage may be pushed off center and caused to lean by simply opening an air entry vane on one side of the cage wider than on the other side. They may be given an S-shape by opening widely the upper right vane and the lower left vane, while leaving the other vanes closed.

When these leaning, or asymmetrical vortices are made visible by means of $TiCl_4$ smoke, they are seen to resemble very closely the tornado in the rope, or dissipating stage. Indeed, the tangential velocity drops very sharply when the vortex is made to lean even a small amount.

Figure 19 gives pictures in alphabetical order to show the effect of causing the fast vortex to be pushed progressively farther off center by using successively greater openings of the lower right vane. Figure 20 portrays a similar sequence for the slow vortex. We see that the vortex becomes progressively more rope-like as it weakens, and as it is pushed farther off center. Note the hollow-tube appearance of the leaning vortex, which differs markedly from the symmetrical vortex, as can be seen by comparison with Fig. 9. Whatever the reason for the tubular appearance, it seems to indicate that the velocity distribution of the leaning vortex is somewhat different in nature from that of the symmetrical vortex. Unfortunately, measurement of these profiles was prevented by the smallness of the velocity. Even with a more sensitive velome-

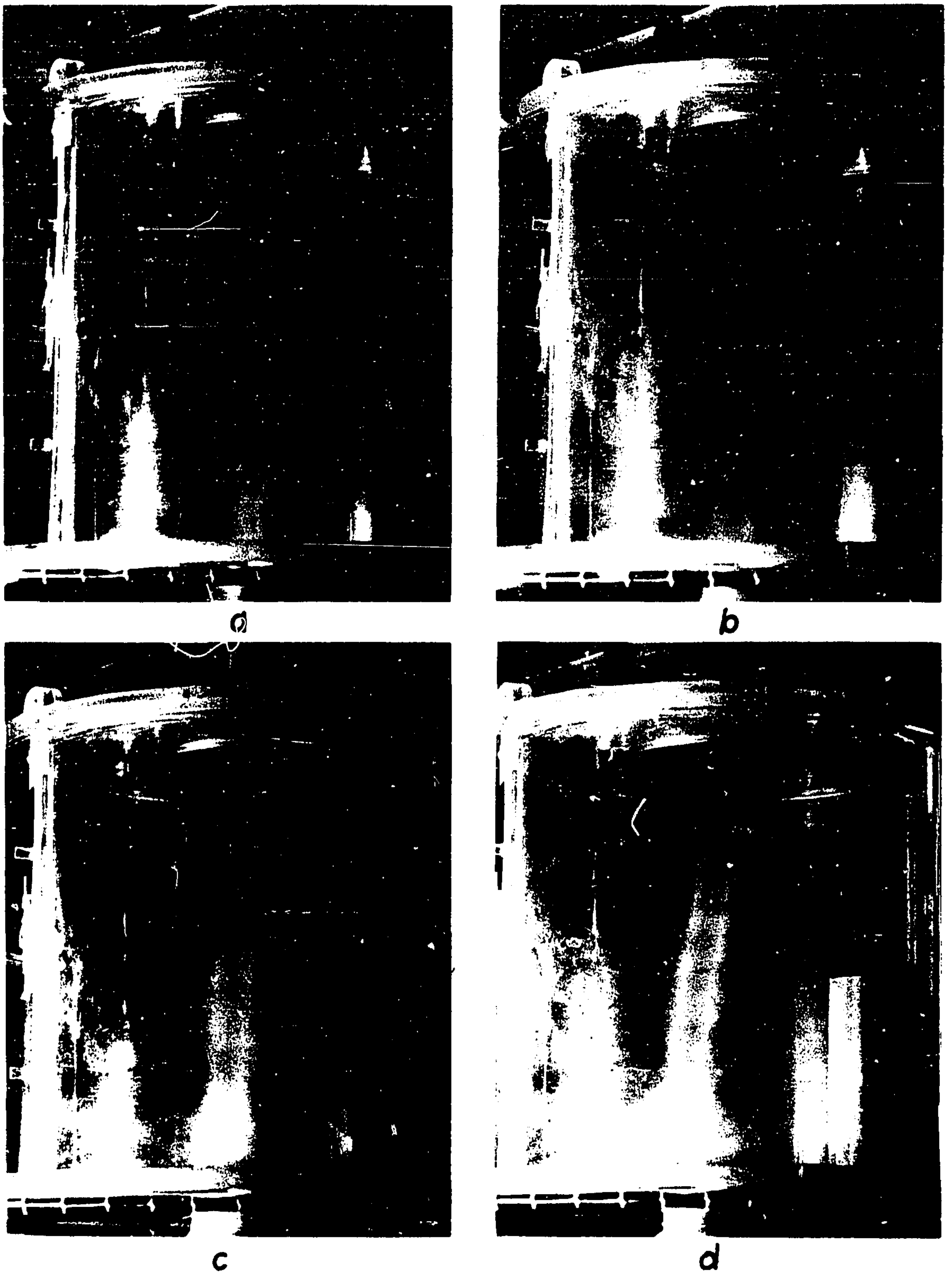

a b c d

Fig. 19. Behavior of the fast vortex as the radial inflow is made progressively more asymmetrical.

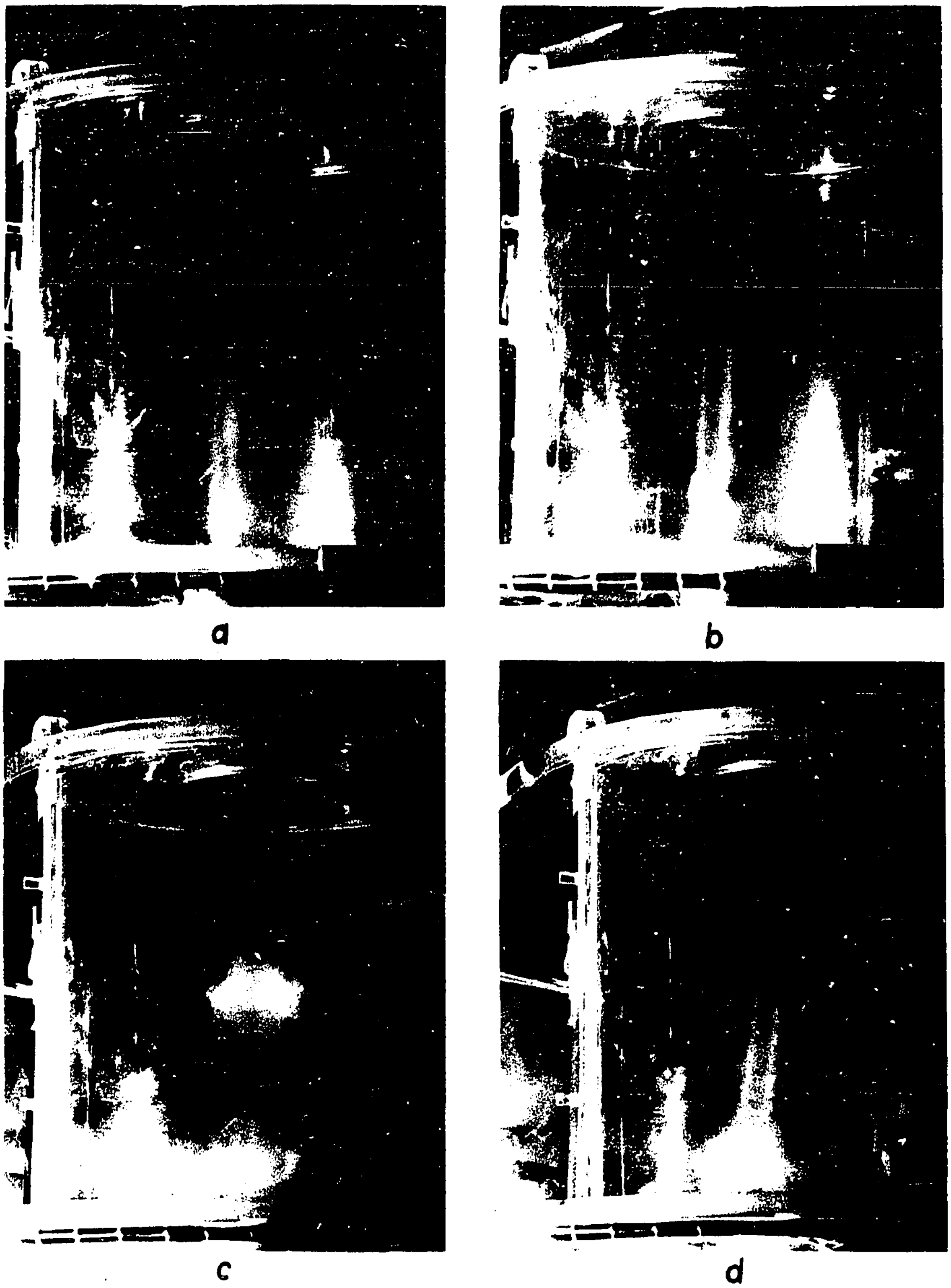

Fig. 20. Behavior of the slow vortex as the radial inflow is made progressively more asymmetrical.

ter it would be difficult to contend with the meandering of the vortex. There must be a greater population of smoke particles in the walls of the tube, but the reason for this is not obvious. Recall that the maximum velocity sleeve has a diameter of 2 in., whereas the outer visible edge has an average diameter of about 1 in.

When the vortex is pushed still farther off center than shown in Figs. 19 and 20, it reaches a stage where the lower end whips about like a loose fire hose. This chaotic motion would be poorly illustrated in a photograph. It occurs when the vortex leans at an angle of about 30 degrees from the vertical. The next stage is a complete vanishing of organized vortex motion, occurring when the vortex is made to lean slightly more than 30 degrees. However, the rope-like tornado has been observed to incline at still greater angles, even approaching the horizontal.

Returning to the complete equations of motion (2) we see that the motion pattern in region II is no longer irrotational when asymmetry terms are added. The motion equations become most complex, even for the simplified vortex model. The vorticity equation (4) gains an asymmetry term and becomes

$$\zeta = \frac{\partial v_\theta}{\partial r} + \frac{v_\theta}{r} - \frac{1}{r}\frac{\partial v_r}{\partial \theta}, \qquad (38)$$

where the latter term represents the asymmetry of radial inflow. As an example, when the circulation is counterclockwise and radial inflow is greatest to the east, then this term makes its greatest contribution to cyclonic vorticity to the north of the vortex, where $\frac{\partial v_r}{\partial \theta}$ is a decreasing function. The vortex would tend to displace in the direction of maximum cyclonic vorticity, or northward in this case.

The lower left photograph in Fig. 20 resembles the double-sleeve tornado, and this situation can be produced also with the centered vortex. When this outer band is present it oscillates up and down the vortex rythmically, contracting as it ascends, and expanding as it descends. The period of the oscillation is about 0.5 sec. This oscillation may be somehow associated with the rythmic surges in tangential velocity very near the vortex axis, which were mentioned in Chapter II.

By combining information from the confinement of the plasma, the visible edge of the $TiCl_4$ smoke, and the observed sleeve of maximum velocity we can construct a cross-section such as Fig. 21. The oscillating outer sleeve of smoke appears to be at a radius of about 1.5 in when it is at mid-height of the vortex, and although it contracts while descending, apparently it never penetrates into the sleeve of maximum velocity.

The Double-Sleeve Tornado

Some tornadoes are also "double-sleeve" vortices, and some information about the structure of these vortices can be obtained by using the model. Both of the sleeves can occur in one region only if the particles making the sleeves visible are of two different densities.

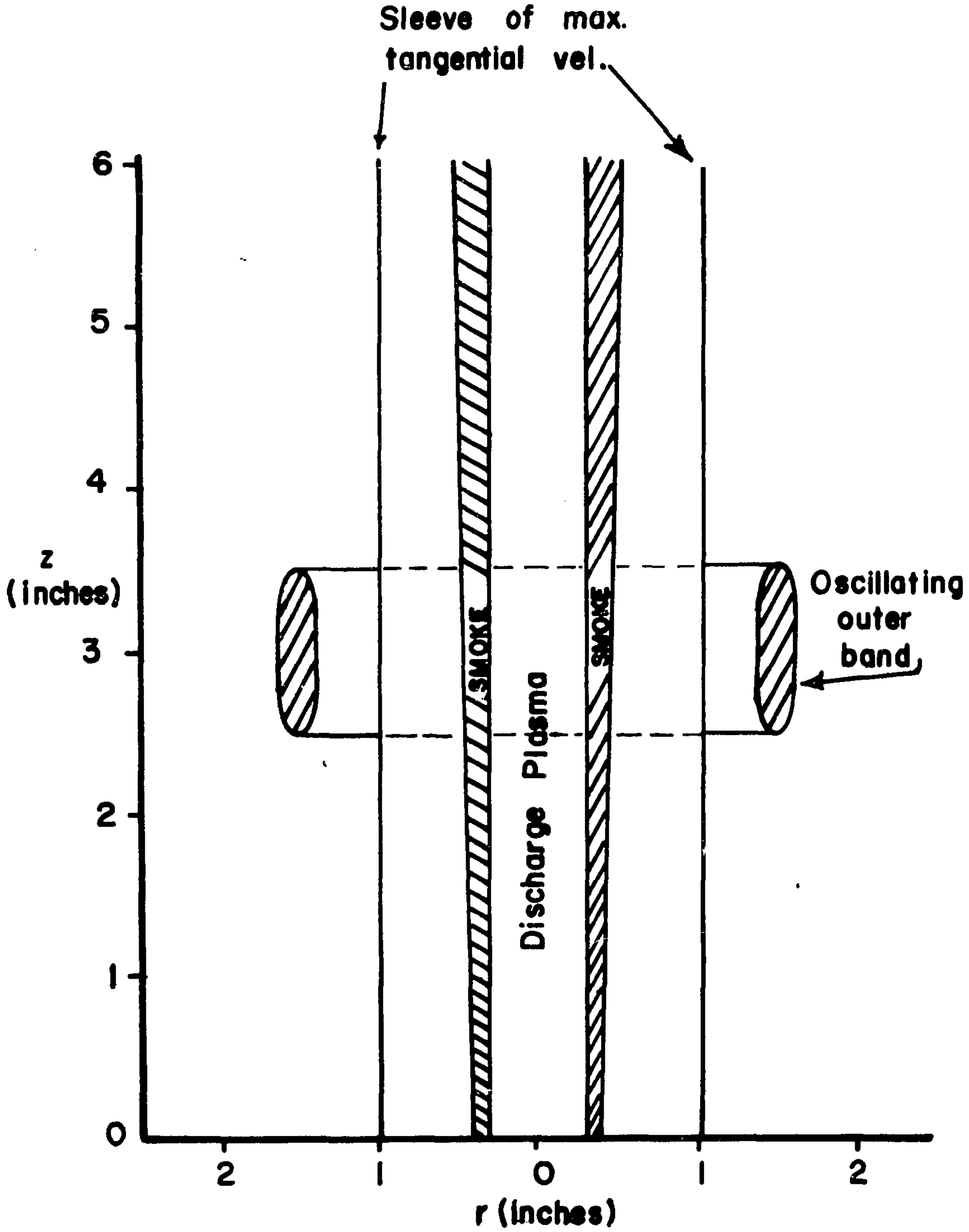

Fig. 21 Cross-section of the laboratory vortex showing boundaries of visible plasma, visible smoke, and sleeve of maximum velocity. Dimensions are true scale.

Such is not the case for the laboratory vortex, and seems very unlikely for tornadoes as well. Let r_1, and r_2 be the radii of the visible sleeves in regions I and II respectively, and ρ' be the density of the particles. Equations for the balance of radial forces in each region can be taken from (7) and (9), and when these are given these notations, we have

$$\omega^2 r_1 (\rho' - \rho) = \left[\frac{\partial p}{\partial r}\right]_1 \tag{39}$$

and

$$\frac{\omega^2 r_m^4}{r_2^3} (1 + K^2) (\rho' - \rho) = \left[\frac{\partial p}{\partial r}\right]_2 , \tag{40}$$

which when combined give

$$\frac{r_m^4}{r_1 r_2^3} (1 + K^2) = \left[\frac{\partial p}{\partial r}\right]_2 \Big/ \left[\frac{\partial p}{\partial r}\right]_1 . \tag{41}$$

The ratio on the right is easily determined to be 0.674 for the laboratory vortex, and this value is satisfactory for the double-sleeve tornado if we have scale model similarity. Ordinarily r_1 and r_2 can be determined photographically, leaving a relationship between the radius of maximum velocity and the K-factor. When r_m can be estimated from the damage path, K can be calculated. If K is measured instrumentally as suggested in Chapter II, then r_m can be calculated. Or, if the optimum laboratory K-factor = 0.36 is used, then

$$r_m = (0.6 r_1 \, r_2^3)^{\frac{1}{4}} . \tag{42}$$

For the laboratory vortex $r_1 = 0.5$ in, $r_2 = 1.5$ in, giving $r_m = 1.0$ in, which agrees with the instrumental determination of r_m.

Chapter IV

CONCLUSION

The results of this research indicate that electrodynamic accelerations will not have a direct influence on either the genesis, maintenance, or intensification of tornadoes. "Direct" influence here refers to vortex motion as a result of accelerations of charges in the electric field of a thunderstorm. It is possible that electrodynamic accelerations play an important role in the charging mechanism, the condensation phenomena, or in the precipitating scheme of convective storms, and in this way these accelerations could have an indirect influence. However, the cloud physics of convective storms is beyond the scope of this paper.

Thermal and aerodynamic effects seem to be the only ones of direct importance to the tornado. The release of heat by lightning alone may drive a weak vortex, but if this release serves to trigger latent-heat convection on an accelerating scale, then it could also be an important factor in tornado genesis. Certainly it seems that the release of condensation and precipitation heat must provide most of the updraft acceleration. The major aerodynamic influence is the organized tangential component of the inflow. This influence is most likely provided by a microcyclone.

Implications toward Tornado Detection and Control

Projecting from these results, it appears that control of condensation phenomena in convective storms would be the most direct approach to tornado control, since control of the aerodynamic action of the microcyclone is very unlikely. Attempts to control condensation by cloud seeding have not met with encouraging results; however only a few seeding agents have been tried, and silver iodide is the usual one. Almost all of the cloud seeding efforts have been conducted in essentially the same fashion, with little ingenuity having been applied along with the enormous financial burden of the effort.

The idea of controlling the electrical phenomena of convective storms has received relatively very little attention, despite the fact that condensation and precipitation may be intimately associated with electrical phenomena in these storms. Even if this were not so, the control of lightning is no less important than the control of tornadoes. Vonnegut and his associates [25], [3], [27] have pioneered in this kind of research. Recently Vonnegut et al.[29] have shown that the electrification of small cumuli may be influenced by seeding with ions from a charged wire. According to Sartor [22] most of the theories of thunderstorm electrification invoke an acceleration of charging due to the presence of the field resulting from the initial charging. If these models are correct, then Vonnegut's method would be most effective if it could be applied in the initiation stage.

The experiments indicate that extinguishing the electrical discharge inside of a tornado could make as much as a 25 per cent increase in the kinetic energy of the horizontal component of motion. This is a measure of tornado control, even though it is not in the direction usually considered desirable.

Plans for Additional Experiments

The experiences of the research program to date suggest further laboratory experiments and theoretical analyses directed toward the problem of tornado detection and control. These experiments and analyses will form the final phase of this program, and will be reported in a subsequent paper.

Preliminary experiments show that the 1280-watt discharge in the laboratory vortex can be extinguished very effectively when seeded with a minute trace of sulfur hexafluoride (SF_6) gas. Furthermore, the discharge cannot be started again until the cage is purged of the gas. This remarkable compound is so stable, insoluble, and such an excellent absorber of negative charge that it seems to be an ideal agent for seeding to prevent or to extinguish electrical discharges in thunderstorms and tornadoes.

Subsequent experiments will be conducted to determine the ideal method for seeding inside of the laboratory vortex and the minimum quantities required to achieve various kinds of results. With this information it may be possible to extend the analysis to cover the seeding of the discharge inside of a tornado.

An additional goal of this program is to investigate the possibility that emanations from the "electrical" tornado could be used to identify and locate the tornado. Presumably the instrumentation for locating this kind of tornado would be similar to the sferics locator, which determines the azimuth of lightning discharges. Vonnegut et al. [28] found that their AC discharge ceased to broadcast when enclosed in a vortex. Earlier experiments in the present program [31] showed that a short DC arc broadcasts as well inside of a vortex as in still air. Preliminary experiments with an 8-in AC arc show an identifiable peak between one and two kc sec^{-1} when the arc is centered in the fast vortex.

The instrumentation used for "listening" is a special receiver driven by a frequency scanner, and connected to an automatic spectrum plotter. The plotter yields a graph of radiated power as a function of the frequency scanned. A special power supply is now under construction with which it will be possible to provide a variable frequency DC discharge over the full length of the laboratory vortex. The frequency spectrum analyzer will also be used with this long DC arc as part of the tornado detection research, since this discharge seems to approximate more closely the type to be expected from thunderstorms.

REFERENCES

1. Battan, L., 1958: Energy of a dust devil. J. Meteor. 15 (2): 235-237.

2. Beckwith, W. B., 1960: Analysis of hailstorms in the Denver network. Physics of Precipitation, Waverly Press, Inc., Baltimore, Md., p. 381.

3. Brook, M., G. Armstrong, R. H. Winder, B. Vonnegut, and C. B. Moore, 1961: Artificial initiation of lightning discharges. J. Geophys. Research 66 (11) : 3967-3969.

4. Brooks, E. M., 1949: The tornado cyclone. Weatherwise 2 (2) : 32-33.

5. Dickson, E. B., 1957: Detection of developing tornado activity. Bull. Amer. Meteor. Soc. 37(10) : 517-518

6. Donaldson, R. J., A. C. Chmela, and C. Shackford, 1960: Some behavior patterns of New England hailstorms. Physics of Precipitation, Waverly Press, Inc., Baltimore, Md., pp. 354-358.

7. Flower, W. D., 1936: Sand devils. Great Britain Meteor. Off. Prof. Notes, No. 71.

8. Fujita, T., 1959: Detailed Analysis of the Fargo Tornadoes of June 20, 1957. Tech. Rept. No. 5, University of Chicago. U. S. Weather Bureau Contract Cwb 9530.

9. Fulks, J. R., 1962: On the Mechanics of the Tornado. N.S.S.P. Report No. 4, U. S. Weather Bureau.

10. Hagenguth, H. J., 1951: The lightning discharge. Compendium of Meteor., Amer. Meteor. Soc., Boston, Mass., pp. 136-143.

11. Hill, M. J. M., 1884: On the motion of a fluid, part of which is moving rotationally and part irrotationally. Phil. Trans., London, A, xxv : 539.

12 Jones, H. L., 1955: Research on tornado identification. Third Quart. Prog. Rept., U. S. Signal Corps. Contract DA-36-039, SC64436, File 421-PH-54-91.

13. Lamb, H., 1932: Hydrodynamics. Sixth Edition, Dover Publications, New York, N. Y., p. 233.

14. Lewellen, W. S., 1960: Magnetohydrodynamically-driven vortices. Proc. 1960 Heat Transfer and Fluid Mech. Inst., Stanford Univ. Press, pp. 1-15.

15. Loeb, L. B., 1939: Fundamental Processes of Electrical Discharges in Gases. John Wiley and Sons, Inc., New York, N. Y., pp. 545-546.

16. Long, R. R., 1958: Vortex motions in a viscous fluid. J. Meteor. 15(1): 108-112.

17. Love, A. E. H., 1893: On the stability of certain vortex motions. Proc. London Math. Soc. 18 (1) : xxv.

18. Lucretius, C. T., circa 60 B. C.: De Rerum Natura. Metrical translation by W. E. Leonard. E. P. Dutton, New York, book 6, p. 206.

19. Mason, B. J., 1957: The Physics of Clouds. Oxford, Clarendon Press, pp. 261-262.

20. Miller, J. E., 1955: A tornado model and the fire whirlwind. Weatherwise 8(4) : 88-91.

21. Rathbun, E. R., 1960: An electromagnetic basis for the initiation of a tornado. J. Meteor. 17(3) : 371-373.

22. Sartor, J. D., 1961: Calculations of cloud electrification based on a general charge-separation mechanism. J. Geophys. Research 66(3) : 831-838.

23. Schonland, B. J. F., 1953: Atmospheric Electricity. Second Edition, John Wiley and Sons, New York, N. Y., pp. 63 and 66.

24. Vonnegut, B., 1960: The electrical theory of tornadoes. J. Geophys. Research 65(1) : 203-212.

25. Vonnegut, B., K. Maynard, W. G. Sykes, and C. B. Moore, 1961: Technique for introducing low-density space charge into the atmosphere. J. Geophys. Research 66(3) : 823-830.

26. Vonnegut, B., and C. B. Moore, 1958: Giant Electrical Storms. (Unpublished research report) A. D. Little Co., Cambridge, Mass., 21 pp.

27. Vonnegut, B., and C. B. Moore, 1960: A possible effect of lightning discharge on the precipitation formation process. Physics of Precipitation, Waverly Press, Baltimore, Md., pp. 287-290.

28. Vonnegut, B., C. B. Moore, and C. K. Harris, 1960: Stabilization of a high-voltage discharge by means of a vortex. J. Meteor. 17(4) : 468-471.

29. Vonnegut, B., C. B. Moore, and others, 1962: Effect of atmospheric space charge on initial electrification of cumulus clouds. J. Geophys. Research 67(10) : 3909-3922.

30. Wilkins, E. M., 1960: Laboratory Investigations of the Relative Importance of Electrodynamic and Aerodynamic Processes in Tornadoes. University of Oklahoma Atmos. Research Lab. project proposal, ARL-1289-1.

31. Wilkins, E. M., 1962:: Laboratory Studies of Electrical-Mechanical Relationships in Vortices. University of Oklahoma Atmos. Research Lab. Report, ARL-1289-2.